FINAL REPORT

Application of Remote Sensing for Fishery Resources Assessment and Monitoring

An Investigation of Skylab EREP Data

October 1975

Department of Commerce
National Oceanic and Atmospheric Administration
National Marine Fisheries Service
Southeast Fisheries Center
Miami, Florida 33149

SEFC Contribution No. 433

MARMAP No. 105

APPLICATION OF REMOTE SENSING
FOR
FISHERY RESOURCES ASSESSMENT AND MONITORING

AN INVESTIGATION OF SKYLAB EREP DATA

Investigation No. 240
Contract No. T-8217B

FINAL REPORT

October 1975

Prepared for Lyndon B. Johnson
Space Center
Houston, TX

Principal Investigator: K. J. Savastano
National Marine Fisheries Service
Southeast Fisheries Center
NMFS Fisheries Engineering Laboratory
National Space Technology Laboratories
Bay St. Louis, Mississippi 39520

Technical Monitor: K. H. Faller
NASA JSC Earth Resources Laboratory
National Space Technology Laboratories
Bay St. Louis, Mississippi 39520

ABSTRACT

Effective management of marine resources is dependent upon reliable data relative to abundance, distribution, and availability of the resource. The availability of this type of data is becoming increasingly important for effective management of the oceanic gamefish resource. Private sportsfishing vessel owners, professional sportsfishing charter boat captains, and state and federal fishery investigators and managers recognize that adequate data about these fish resources are the cornerstone for establishment of a sound resource management program. The NASA Skylab/EREP program provided an opportunity for a joint effort among sportsfishermen, industry and the government to increase understanding of the gamefish resource through application of advanced remote sensing technology.

The investigation was initiated in June, 1973, with the field operations phase conducted on August 4 and 5, 1973, in the northeastern Gulf of Mexico. This joint effort by private and professional fishermen, and NASA and NOAA/NMFS elements, was undertaken to acquire synoptic fishery and oceanographic data in association with near simultaneously acquired Skylab-3 and aircraft remotely sensed environmental data.

The primary objective of the investigation was to evaluate the potential of using satellite and aircraft acquired remote sensing data to determine the availability and distribution of oceanic gamefish. This objective was explored through a series of correlations among aerospace (satellite/aircraft) imagery, spectrometry, and sea truth information related to the marine environment and the gamefish resource. Available Skylab and aircraft underflight data were analyzed in conjunction with sea truth oceanographic measurements and oceanic gamefish distribution data from the 5,400 square nautical mile study area in the northeast portion of the Gulf of Mexico. This was done to demonstrate relationships between 1) select oceanographic parameters and oceanic gamefish distribution, 2) aerospace data and oceanographic parameters, and 3) aerospace data and oceanic gamefish distribution.

Oceanographic sea truth and meteorological parameters utilized in correlation analyses were depth, sea state, distance from shore, chlorophyll, sea surface temperature, salinity, water transparency, water color, surface atmospheric pressure, and surface air temperature. Subsets of the above parameters which correlated significantly with distribution data on selected gamefish species were used in the development of oceanic gamefish distribution prediction models. Independent test data were used to provide limited model validation.

An additional model was developed from sea surface temperature and radiance values from bands 2, 3, 6, and 7 of the Skylab S192 multispectral system. This model showed significant improvement over the models developed, for the same time period, solely from sea truth parameters.

ACKNOWLEDGEMENTS

The Skylab Oceanic Gamefish Project was a lengthy, multidisciplined experiment entailing an extensive data gathering operation followed by a complex and detailed data analysis phase. In any such experiment it is difficult to focus on individual efforts. However, each role was important and the Principal Investigator gratefully acknowledges the efforts of the many participating organizations and individuals who contributed to the experiment.

Sportsfishermen provided gamefish data resulting from participation in a tournament coordinated through the Pensacola Big Game Fishing Club by a committee of anglers representing four big gamefishing clubs and two charterboat associations. The committee members were Mr. G. Arnold III, Mobile Big Game Fishing Club, Mr. Bill Bacon, Destin Charter Boat Association, Mr. M. Claverie, Jr., New Orleans and Golden Meadow Big Game Fishing Clubs, Dr. F. T. Neth, Pensacola Big Game Fishing Club and Mr. B. J. Putnam, Panama City Charter Boat Association. Another contribution from the sportsfishing community was the use of facilities at check point marinas at Pensacola, Destin and Panama City, FL, during field operations.

The National Aeronautics and Space Administration's (NASA) Lyndon B. Johnson Space Center (JSC), Houston, TX, directed the activities of the Skylab astronauts during overpass, provided the earth survey aircraft, the NC130B, to overfly the test site, and contracted the experiment. The NASA National Space Technology Laboratories (NSTL) (formerly Mississippi Test Facility), Bay St. Louis, MS, provided extensive laboratory, field site and public relations support. The NASA contractors at NSTL, the General Electric Company and Lockheed Electronics, Inc., assisted with field and technical support. Particularly, I want to acknowledge the efforts of Mr. H. Holley and Mr. G. Stephenson of General Electric for computer programming support; Mr. J. Brashier of Lockheed for data processing support; and Mr. J. Bettens and Mr. B. Braud of General Electric for assistance in preparing reports.

The NASA JSC Earth Resources Laboratory (ERL) located at the NSTL was responsible for the planning, acquisition and processing of surface and remote oceanographic data. Mr. E. L. Tilton, NASA ERL, and his successor as technical monitor, Dr. G. C. Thomann, provided guidance. Mr. J. W. Weldon, now NASA JSC, as a co-investigator did much of the operational planning and execution with Mr. K. Faller, NASA ERL, assuming the responsibilities of Mr. Weldon after the latter's departure. Mr. Faller contributed significantly to the analysis segment of the experiment in the area of remotely sensed oceanographic data correlation to the environment.

The U.S. Air Force provided DAPS satellite data received at Keesler AFB, MS, and a U.S. Navy representative from the Environmental Prediction Research Facility, Monterey, CA, assisted in the analysis of the DAPS data. Weather data was also received through the National Environmental Satellite Service from the NOAA-2 satellite. The weather station at Eglin AFB, FL, launched a special radiosonde coincident with Skylab overpass to provide meteorological data.

Test site safety measures were coordinated with the U.S. Naval Air Station, Pensacola, FL, and the U.S. Coast Guard Headquarters at Mobile, AL. The Coast Guard Station on Santa Rosa Island, FL, provided logistics support during field operations.

The National Oceanic and Atmospheric Administration's (NOAA) National Marine Fisheries Services (NMFS) laboratories at NSTL, Pascagoula, MS, Panama City, FL, and the Southeast Fisheries Center (SEFC), Miami, FL, provided management and technical direction for the experiment as well as field and sampling support. Mr. Harvey R. Bullis, Center Director, Southeast Fisheries Center, provided overall guidance and technical direction to the experiment. Mr. W. H. Stevenson, now at NMFS Southeast Regional Office, St. Petersburg, FL, organized and managed the experiment as the initial Principal Investigator at the NMFS Fisheries Engineering Laboratory (FEL) at NSTL. Dr. Andrew Kemmerer, Director of Technology Division Southeast Fisheries Center, assisted in editing of final report. Mr. E. J. Pastula, Jr., NMFS FEL, as a co-investigator, contributed to operations. Mr. P. C. Cook, NMFS FEL exercised budgetary control throughout the experiment. Mr. L. Rivas, NMFS Panama City, functioned as a liaison with gamefishing sportsmen and charterboat captains. Mr. E. G. Woods, NMFS FEL, planned and coordinated field operations on 4 and 5 August 1973.

TABLE OF CONTENTS

TABLE OF CONTENTS (CONT'D)

TABLE OF CONTENTS (CONT'D)

LIST OF ILLUSTRATIONS

TABLE OF CONTENTS (CONT'D)

LIST OF TABLES

TABLE OF CONTENTS (CONT'D)

SECTION 1

INTRODUCTION

1.1 REPORT REQUIREMENT

This document is the final report required under NASA Contract No. T-8217B for Skylab EREP Investigation No. 240 entitled "Application of Remote Sensing for Fishery Resources Assessment and Monitoring". The report covers the period of contract performance from 20 April 1973 to 30 October 1975. In addition to this final report, a series of monthly progress reports (1) have been submitted since inception of the experiment.

1.2 PROJECT SUMMARY

The project was contracted to the National Marine Fisheries Services (NMFS) Southeast Fisheries Center, Fisheries Engineering Laboratory (FEL) by the National Aeronautics and Space Administration's (NASA) Lyndon B. Johnson Space Center (JSC). However, many elements of the National Oceanic and Atmospheric Administration (NOAA) and NASA participated. The NASA JSC-Earth Resources Laboratory (ERL) located at the National Space Technology Laboratories has had responsibility in the planning, acquisition, and processing of surface and remote oceanographic data required to meet the experiment objectives. The laboratory's role was defined in NASA document (2).

After contract receipt, a program plan (3) was prepared and issued which included technical direction, schedules, data requirements and management instructions. Coordination was effected through a series of project review meetings which were held daily during the most intense planning period for field operations.

Field operations were conducted 1 through 3 June and August 4th and 5th 1973, but the earlier operations were limited in scope. There was no Earth Resources Experiment Package (EREP) participation during the June operations and the earth survey aircraft overflight was cancelled. In addition, poor fishing conditions resulted in the acquisition of meager catch data. A review of all acquired data revealed an insufficiency of data on which to base meaningful analysis. The June operation was, however, useful as a rehearsal for the August operations.

The 4 and 5 August operations (4) resulted in a much improved data acquisition performance even though the Skylab EREP overpass occurred during a period of 40-70% cloud cover. Fortunately the NASA aircrafts' overflights occurred hours earlier with sensor arrays operating in better weather. Observers in nine oceanographic research vessels obtained sea measurements over the two-day period and hundreds of saltwater anglers, sportsfishing boat owners and charterboat captains voluntarily contributed resource catch data. An overview of the operation is shown in Figure 1. Participants are listed in Table 1.

The project entered the final or analysis phase following the August field operations. Data preparation functions, e.g., review, transposition, keypunch and verification, for environmental and fisheries data consumed the initial portion of this phase. The file was completed

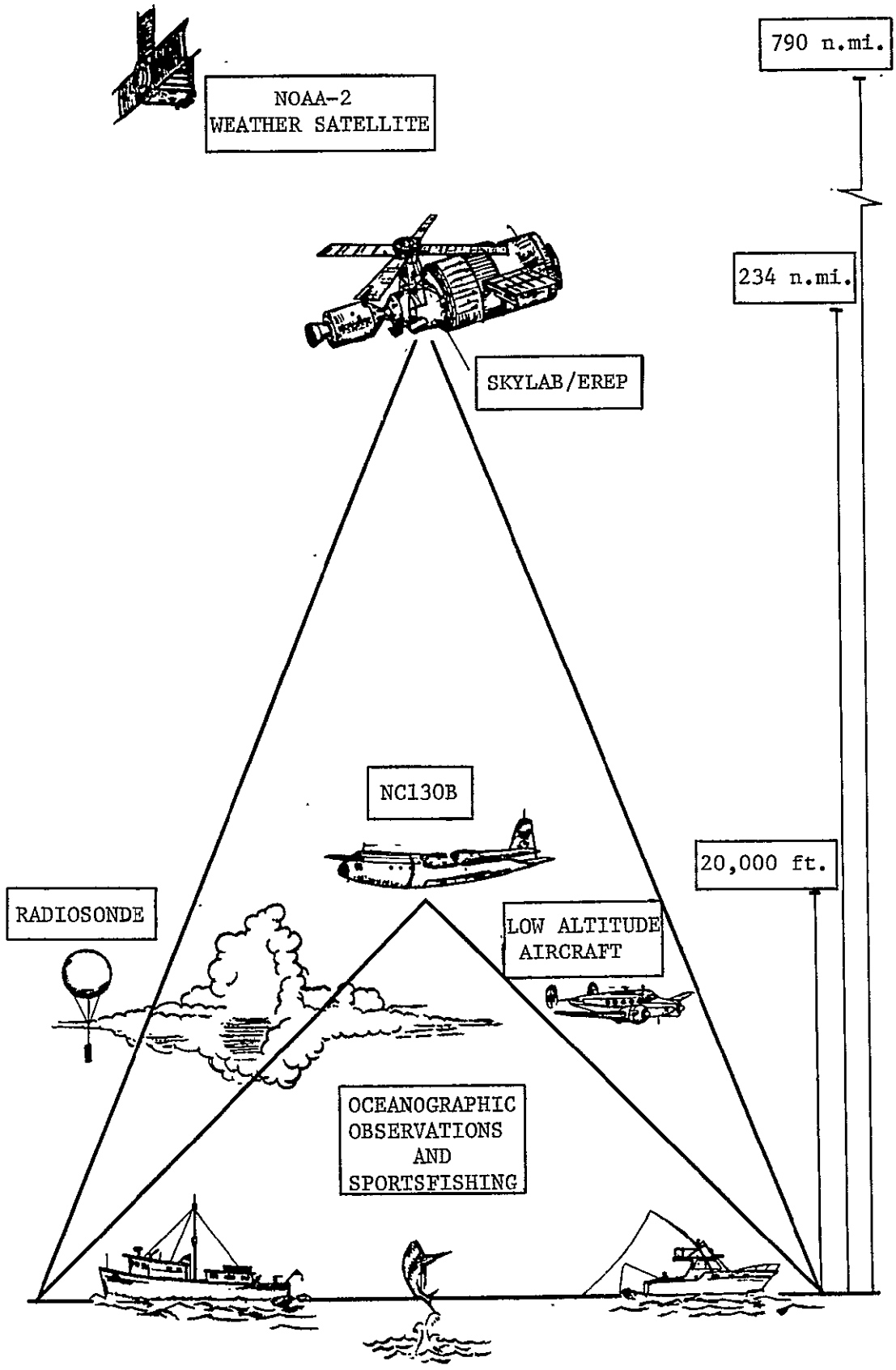

Figure 1. Operational Overview

Table 1. Participants

GOVERNMENT AGENCIES		SPORTSFISHING
NOAA	NASA	
National Marine Fisheries Service	Johnson Space Center	Panama City Charterboat Association
National Environmental Satellite Service	Earth Resources Laboratory	Destin Charterboat Association
National Weather Service	Goddard Space Flight Center	Pensacola Big Game Fishing Club
National Ocean Survey	OTHER	Mobile Big Game Fishing Club
	U.S. Air Force	New Orleans Big Game Fishing Club
	U.S. Navy - EREP WRCON/JAX	Golden Meadow Big Game Fishing Club
	U.S. Coast Guard	

about mid-October 1973. A partial mailing of remote sensing products was received in September followed by intermittent receipts through the remainder of the analysis phase. Numerous analyses were undertaken through May 1974 relative to the correlation of the resource with the environment, the inferrence of oceanographic parameters from remotely sensed data and the development and test of predictive models.

1.3 OBJECTIVES

The primary objective of the investigation was to establish the feasibility of utilizing remotely sensed data acquired from aircraft and satellite platforms to assess and monitor the distribution of oceanic gamefish. This was explored through a series of correlations among aerospace (satellite/aircraft) imagery, spectrometry, and sea truth information related to the marine environment and the gamefish resource.

Additional objectives of the experiment were to:

- Examine relationships between ocean surface data and gamefish distribution
- Enhance capability to predict best areas for gamefishing success

1.4 FISHERY RESOURCE

The target resource, oceanic gamefish, included the following species for this experiment.

Blue Marlin, Makaira nigricans
White Marlin, Tetrapturus albidus
Sailfish, Istiophorus platypterus
Wahoo, Acanthocybium solanderi
Dolphin, Coryphaena hippurus
Yellowfin Tuna, Thunnus albacares
Bluefin Tuna, Thunnus thynnus

Oceanic gamefish were selected as the focal point of the experiment on the following premises:

- Relatively little is known concerning the status of billfish, either from a commercial or a sportsfishing point of view (5).
- Gamefish constitute a major source of recreation for an increasing number of saltwater anglers.
- The resource is being exploited by the Japanese longline fishery and there are indications (6) that the fishing intensity has reached or exceeded that level beyond which a maximum annual yield cannot be sustained.
- Skylab EREP Program offered, through remote sensing techniques, an unusual opportunity to make a significant advance in knowledge of the relationship between oceanic gamefish and their environment. The knowledge could be applied in the development of new marine resource management techniques.

1.5 EXPERIMENTAL APPROACH

Resources permitted no more than two missions of several days each for data acquisition. As a matter of prudence in allocating the budget, it was decided to emphasize the second mission (4-5 August) utilizing the lessons learned in a first, less ambitious mission.

It was clear from the outset that mission success, specifically the acquisition of fish catch data, depended on the voluntary, enthusiastic cooperation of sportsfishermen. Accordingly, a vigorous sportsfishermen relations program was initiated with the objective of enlisting their wholehearted support. The Principal Investigator met with the sportsfishermen to explain the cooperative project and a framework for their participation was established. With interest aroused, additional measures were taken to sustain the interest through the second mission.

Redundancy was planned in the selection of remote sensors in order to minimize adverse effect on the experiment due to the non-availability of a platform, sensor malfunction, etc., however, a total overlap was impossible. Skylab EREP sensors' footprints were far wider than those of the aircraft sensors, and the capabilities did not provide adequate coverage in

other respects. For example, no aircraft sensor was available in this experiment for remote measurement of salinity and Skylab EREP S194 sensor resolution for remote measurement of salinity was too gross to meet requirements.

Acquisition of environmental data above that obtainable from the Government and contract oceanographic vessels was increased by placing oceanographic observers on selected sportsfishing boats. This resulted in the coverage of a larger area and a good correlation between the additional data and the gamefish catches. The net effect was an improved surface platform data acquisition plan within the available budget.

The analytical approach (described in detail in Section 6) was to define the relationship between the resource and the environmental parameters, infer oceanographic information from the remotely sensed data and then relate the remotely sensed data to the resource. It was then determined through model development and evaluation, if the relationship had meaning in terms of resource utilization management.

SECTION 2

TEST SITE

2.1 DESCRIPTION

The test area (Figure 2) for the August operation comprised 18,000 square kilometers and was shaped roughly like a triangle, bounded by the coordinates 30°16'N, 86°51'W, 29°18'N, 85°47'W; and 29°21'N, 87°56'W on the north, east and west, respectively. The northern apex lay 14 kilometers south of Santa Rosa Island and the southern serrated edge extended 155 km south of the apex. The sides extending from the northern apex approximated the 55 meter curve along the coast. The northern extremity of the De Soto Canyon lay within the southern portion of the area providing depths in excess of 1600 meters. In order to provide a grid for referencing gamefish catches, the fishing area was divided into 54 squares with 18.3 km (10 nautical miles) to a side. Skylab track 62 approximately bisected the area, extending southeast from Mobile Bay.

The June exercise utilized a much smaller area made up of only 36 fishing squares. Because of the lack of gamefishing success during the early summer months, it was decided to expand the fishing area further offshore for the August operation in hopes of finding "blue" water. The rationale was that better gamefishing was associated with offshore "blue" water as compared to inshore "green" water.

2.2 SELECTION CONSIDERATIONS

The northeastern Gulf of Mexico in the vicinity of the De Soto Canyon is noted for a relative abundance of oceanic gamefish during the summer season. Also, hundreds of sportsfishing boats are based in numerous marinas along the coast and it was anticipated that owners, charterboat captains and anglers would cooperate in providing volunteer catch data. Several gamefishing clubs and charterboat associations were headquartered in nearby cities, simplifying communications relative to the field experiment.

Management and logistics were facilitated by the proximity of the Fisheries Engineering Laboratory and the Earth Resources Laboratory at the National Space Technology Laboratories, Bay St. Louis, Mississippi. The test site was also conveniently close to the supporting NMFS laboratories at Pascagoula, Mississippi, and Panama City, Florida.

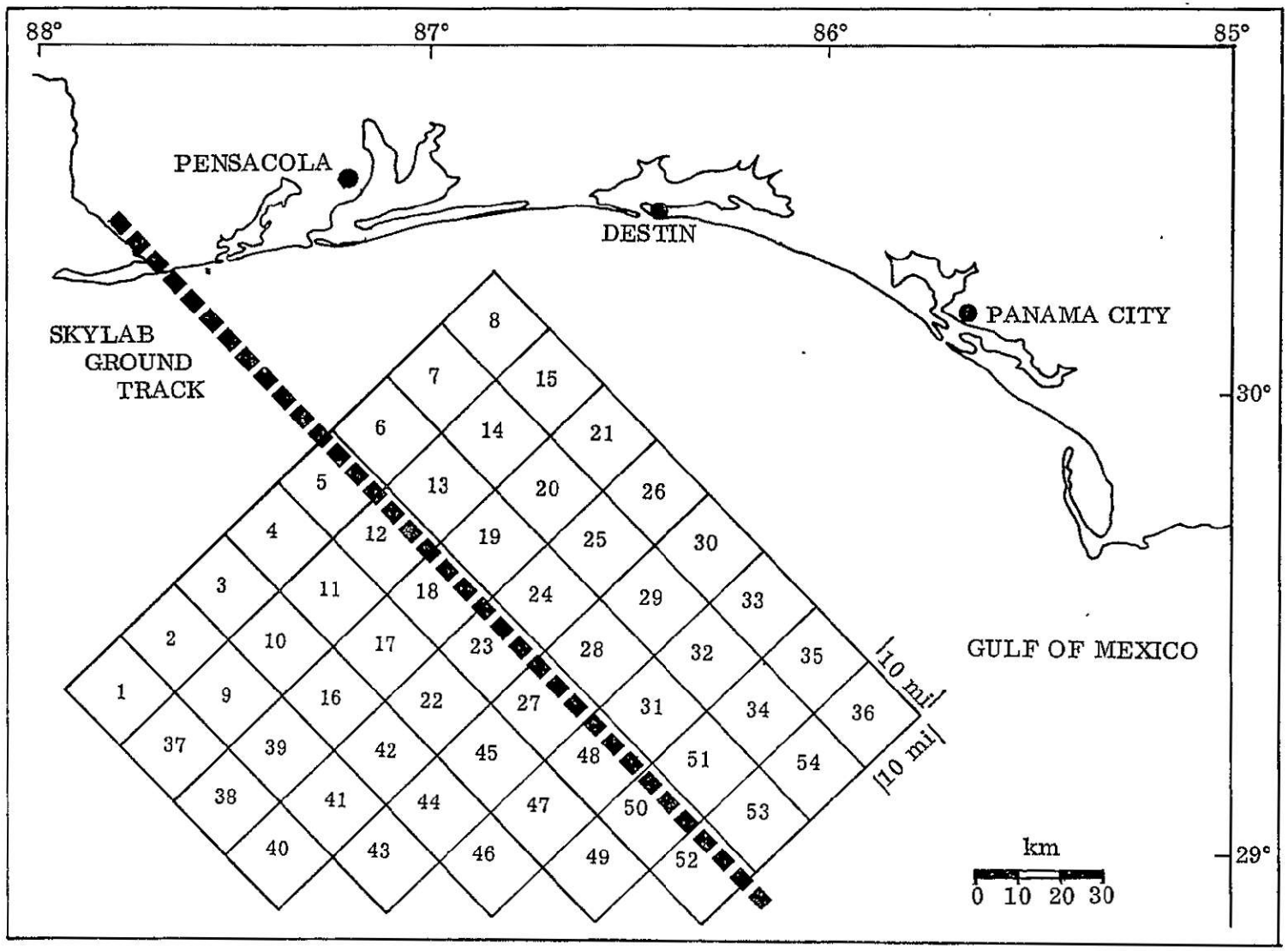

Figure 2. Test Area with Fishing Squares - 4-5 August Mission

SECTION 3

DATA SYSTEM

3.1 MANAGEMENT

Early in the Skylab experiment a data management plan was implemented which covered the entire system of data acquisition, data collection, and subsequent data processing. The first step of the plan was to identify the data requirements during project review meetings (Figure 3) and evaluate the requirements to determine their applicability to the project objectives. Each requirement was further reviewed to:

- Determine the acquisition, processing and analysis responsibility
- Identify conflicting and redundant requirements
- Determine schedule requirements
- Establish priority, data control factors, and responsibilities

Approved data acquisition requirements were then assigned to the agency with the designated responsibility and recorded in the program plan (3).

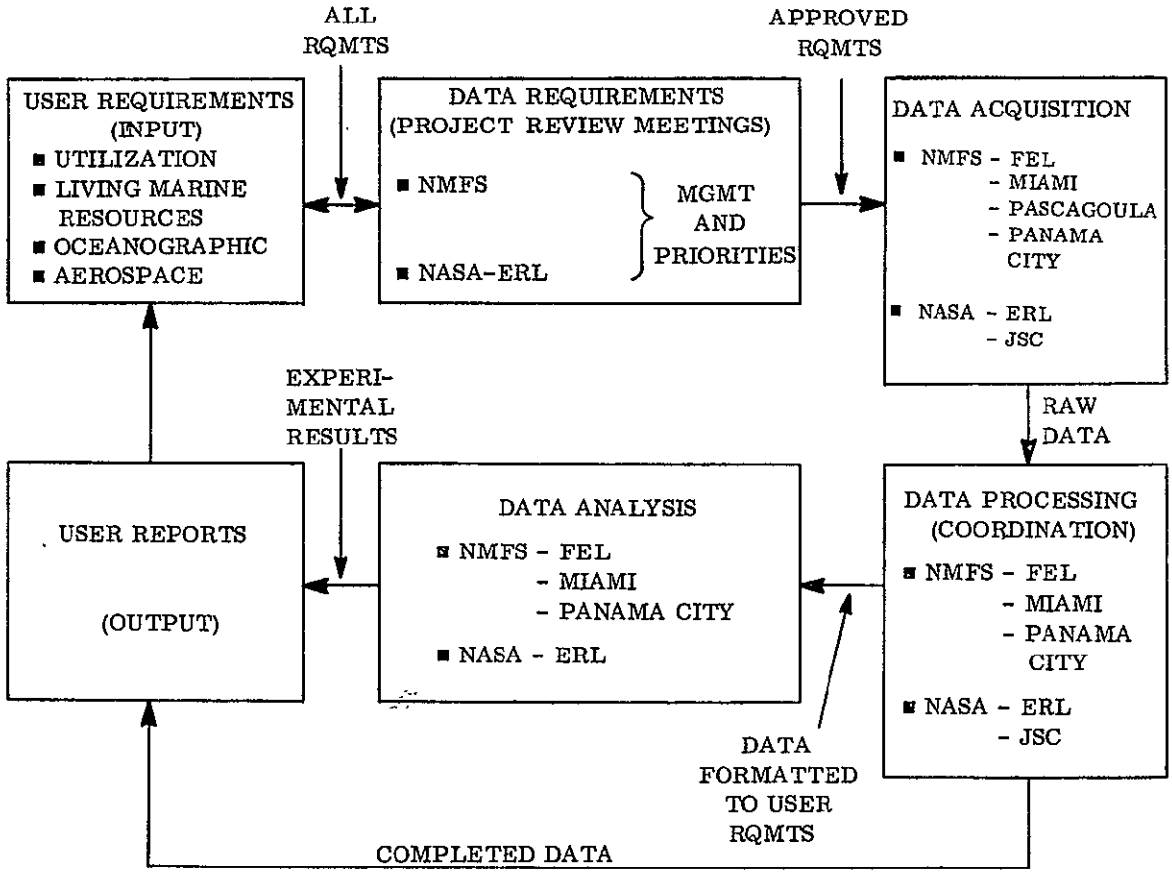

Figure 3. Data Management Flow

A FEL Data Processing Coordinator was designated as the focal point for all processing requirements. The Coordinator's responsibilities included providing adequate information to the processing agency to ensure performance within the established constraints; monitoring activities to provide visibility for incoming raw data, processing tasks and analysis schedules; and assuring that reproduction and other supporting functions were available as required.

All NMFS FEL processing of project data was handled by the FEL Data Processing Coordinator (Figure 4) who received, logged, and prepared all incoming data for the next phase of processing. A master file of all data was established by FEL and the data was furnished to users upon their request. Following the data acquisition phase, an Interim Data Report (7) was issued to inform prospective users of the data available. The report included listings of sea truth and fisheries data, and point and contour plots acquired on the 4 and 5 August mission.

3.2 EQUIPMENT

All computer processing was performed on the Univac 1108 EXEC VIII multiprocessing system located at the NASA Slidell Computer Center. A complete system diagram is depicted in Figure 5. The SC-4020 microfilm printer/plotter and Xerox Copyflo printer were also used extensively during the project to provide visual displays and to report data and information to be utilized by the analysis group.

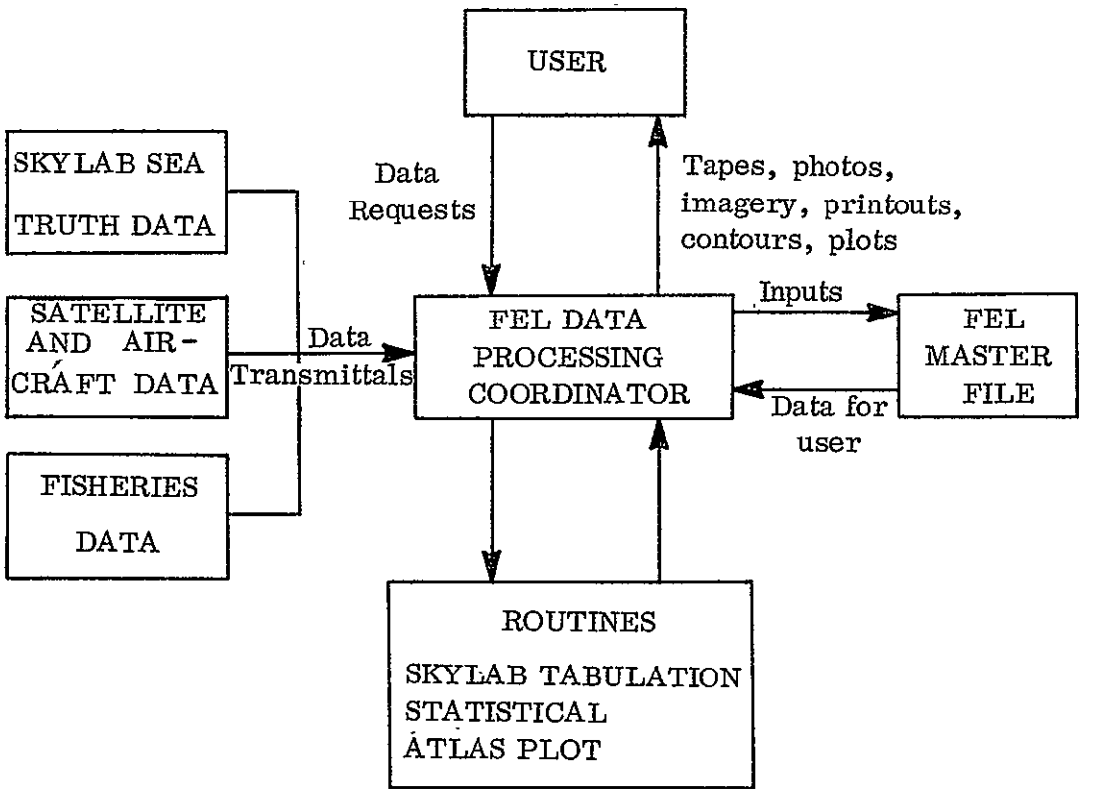

Figure 4. Data Processing Overview

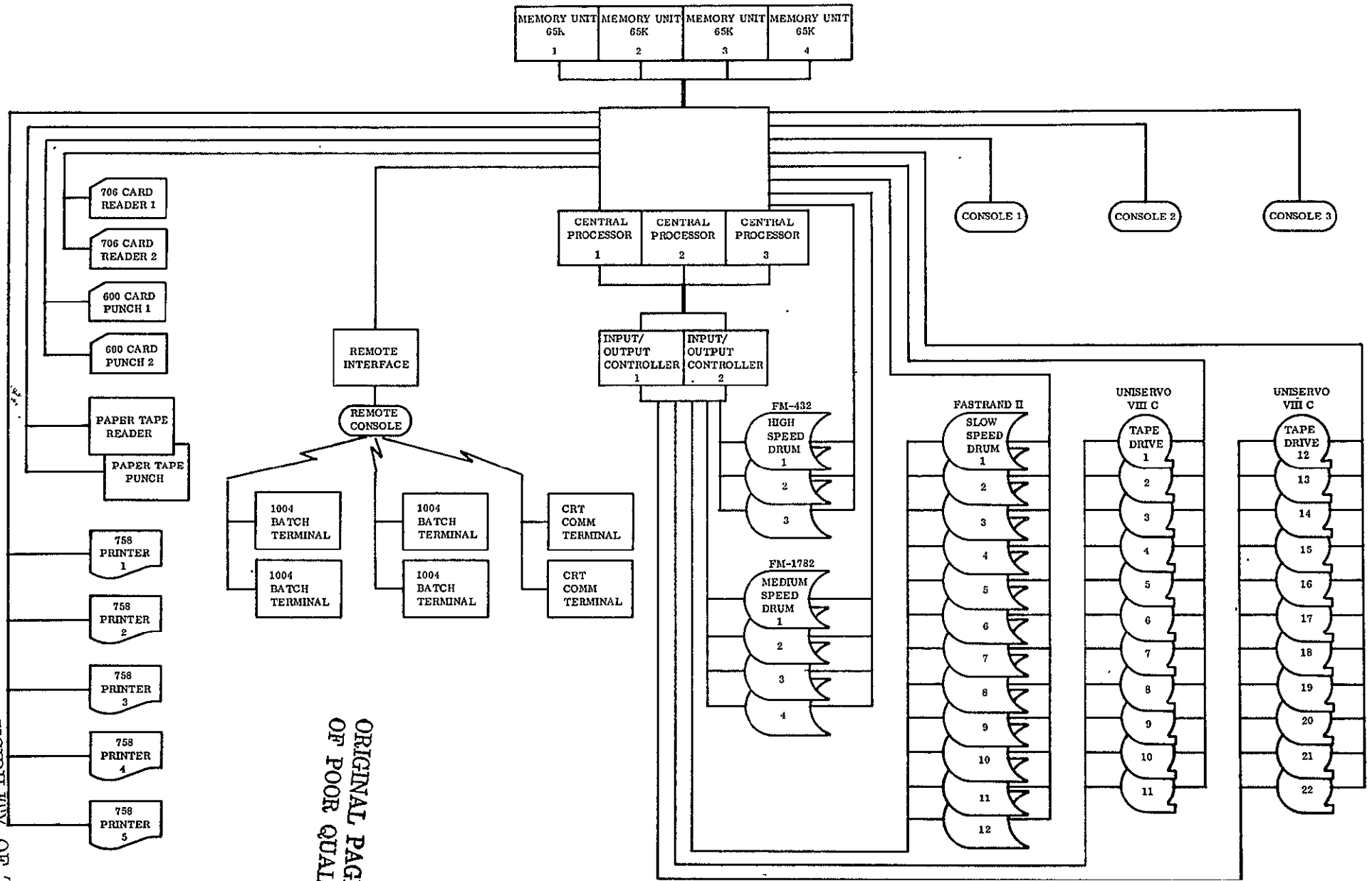

Figure 5. Computer System

3.3 SOFTWARE

In addition to the EXEC VIII system software, compilers, library routines, and special processor, statistical routines were available and several were modified for application to the Skylab data. The step-wise multiple regression routine was used extensively in model development tasks.

Application software to establish, maintain, and utilize the Skylab data consisted of three main segments (Figure 6). The first segment was used to convert the various measurement parameters to standard units and format. The output of this program, binary coded decimal magnetic tapes, was used along with card definition of the data as input to the Information Storage and Retrieval System (ISRS). The compressed data banks were built utilizing the UNIVAC 1108 computer and ISRS. The system provides for simple English language commands which enabled the users to selectively retrieve information subsets from the compressed files, print the information, or store it on magnetic tape to be utilized by upstream analysis programs. The system has the capability of locating information in the Data Bank, satisfying given search criteria by mathematical calculation rather than by sequential searching. This segment was used in the early stages of analysis to selectively retrieve subsets of information which were used in the decision processes. The last segment consists of several computer programs developed by FEL at NSTL to analyze and display the selectively retrieved information subsets. The system provides software for statistical analyses such as data grouping, moment computations, arithmetic mean, standard deviation, linear and multiple regression, discriminant function, etc.

Specialized software was prepared to perform similarity/ordination analyses and various mathematical computations. The Atlas Display System (ADS), a graphical display system, was utilized to display biological, oceanographic and meteorological data at the proper latitude/longitude and to display any land masses which are applicable to the location.

3.4 SEA TRUTH ENVIRONMENTAL DATA

Environmental data acquired from surface platforms were processed by NASA ERL. ERL designed and distributed the environmental raw data collection logs (Appendix A), provided instruction on their use, and collected and completed logs after the mission. They also provided the data keypunch and furnished one card deck to the FEL Data Processing Coordinator for input to the Skylab Master File and preparation of quick look plots.

3.5 FISHERIES DATA

Fisheries data in raw form were collected from sportsfishermen and recorded on the Gamefish Boat Log (Appendix A). The initial format for the log was approved by the Government's Office of Management and Budget. The logs were collected and completed by port samplers when the gamefishing boats stopped by the check points in the late afternoon. The completed logs were sent to FEL for data-transposing to load forms, editing, keypunching and input into the Master File.

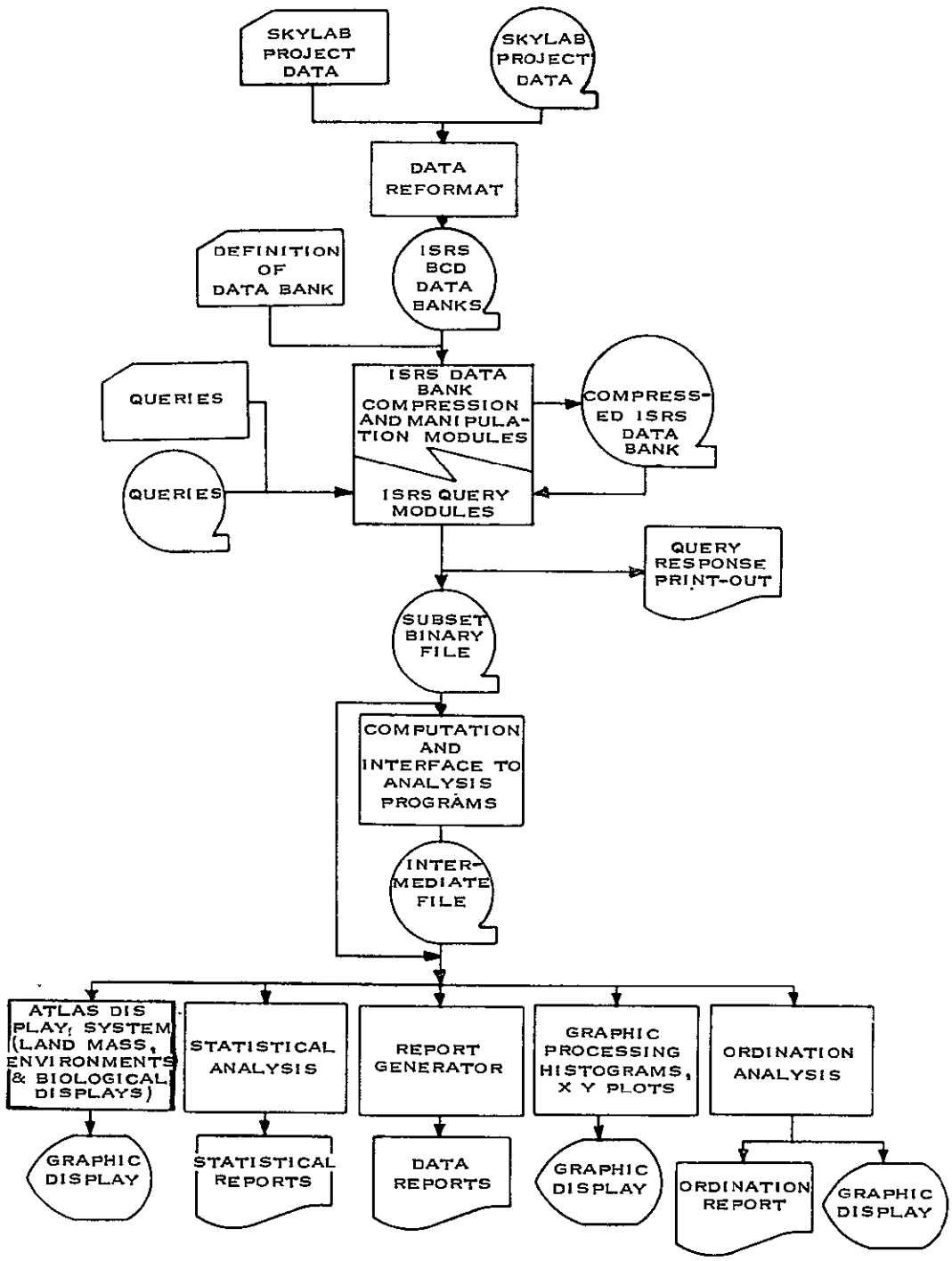

Figure 6. Data Management Software System

3.6 SKYLAB ACQUIRED DATA

Skylab acquired data products were requested by use of the Investigation Requirements Document. The request was processed through the NASA JSC as described in NASA document (8). After receipt in the office of the Principal Investigator, all remotely sensed data products were reviewed, logged, and then made available to the NASA ERL for analysis in inferring oceanographic parameters and subsequent archiving. Satellite remote sensing product receipts are listed in Appendix B.

3.7 AIRCRAFT ACQUIRED DATA

Data acquired by the NC130B aircraft were processed by the NASA JSC which was furnished product requirements by means of the NASA "Project Requirements for Aircraft Support" document. Subsequent to field operations, the Principal Investigator was afforded a quick look of the photograph products in Houston and provided the opportunity to modify the previous request. NASA ERL processed data acquired by the NASA contracted E-18 aircraft and furnished data products to requesters as determined in project review meetings and recorded in the project plan (3). Aircraft remote sensing product receipts are listed in Appendix B.

3.8 DATA FORMATS

Data format requirements with scheduled availability, formatting agencies and users were developed as shown in Table 2.

3.9 DATA ARCHIVING

All aircraft and Skylab sensor film and tape products received in the project have been retained in the NASA ERL for continuing study and storage. A log of all product receipts from the NASA JSC has been filed by FEL.

The load form originals for sea truth environmental data were stored by NASA ERL. The boat logs, load forms and card decks by which the fisheries data were obtained and processed were filed by FEL. Magnetic tapes of environmental and fisheries data were stored at the NASA Slidell Computer Center. Copies of these magnetic tapes along with their format and data description were forwarded to the National Oceanographic Data Center for archiving.

Table 2. User Data Formats

DATA	USER DATA FORMAT	DATA AVAIL.	FORMAT AGENCY	USERS
Surface Acquired	Punched Cards	2 wks.	ERL	FEL
Oceano and Met.	QL Plots	3 wks.	FEL	Miami (2), Pascagoula, ERL
	Final Plots	10 wks.	ERL	FEL, Miami (2), Pascagoula
A/C Acquired	Film	12 wks.	ERL	Original Available for Viewing
NC130B	Punched Cards MSS Ch. 2-7 Radiance Value, ev. 5 n. mi., 2-1/2 n. mi. each side of centerline, long. and lat. of data points	12 wks.	ERL	FEL
A/C Acquired	File of T° profile.	8 wks.	ERL	Original Available for Viewing
E-18	Final plots RS-18 Thermal Digital Map with T° marked ev. 5 n. mi.	8 wks.	ERL	FEL, Miami (2), Pascagoula
	Punched cards on above RS-18 data with location data.	8 wks.	ERL	FEL
	Punched cards E 20-D spectrometer radiance values, 0.4-0.75 μm range ev. 50 nanometers with location data.	8 wks.	ERL	FEL
Skylab Acquired	Film	8 wks.	ERL	Original plus 4 copies
	Punched cards, S191 radiance values, 0.4-0.7 μm range ev. 50 nanometers	10 wks.	ERL	FEL
	S192 Ch. 1-6, grey scale, 0-255 count	10 wks.	ERL	FEL
	Punched cards S192 with digital count for centers of area grid and subsets	10 wks.	ERL	FEL
	S192 thermal map, grey scale with digital printout ev. 5 n. mi. with location data	10 wks.	ERL	FEL, Miami (2), Pascagoula
Fisheries	Punched cards	2 wks.	FEL	Miami

SECTION 4

PARAMETERS

4.1 SELECTION

As described in Section 3, the selection of parameters to be measured during data acquisition was coordinated among the participants during project review meetings and later documented in the program plan. At the same time, measurement tolerances were agreed upon. Generally there was acceptance of a parameter and associated tolerance if the proponent affirmed that the requirement existed in order to perform the analysis necessary to meet experiment objectives.

The susceptibility of all parameters to remote measurement was unclear at the time of selection but it appeared evident, from ongoing experience, that values could be inferred for sea surface temperature (9) (10), chlorophyll (11), turbidity (12) and salinity (13) from remote sensing.

4.2 ENVIRONMENTAL PARAMETERS

The requirements for environmental parameters are shown in Table 3. Measurement and recording procedures for sea truth values are described in NASA document (2).

4.3 FISHERIES PARAMETERS

The requirements for fisheries parameters are shown in Table 4.

Table 3. Environmental Parameter Requirements

MEASUREMENT	ACQUISITION UNITS	ACCURACY	FINAL CONV
Sample Time	2400 Clock	1 minute	———
Surface Water Temperature	°C	.1°C	———
Surface Water Salinity	ppt	.01 ppt	———
Air Temperature	°C	.1°C	———
Wet and Dry Bulb Pyschrometer	Degree	1 degree	———
Wind Direction	Compass Point (N, ENE, NE, etc.)	———	———
Wind Speed	mph	1 mph	km/hr.
Secchi Depth	feet	1 ft.	m
Sea State	feet	1 ft.	m
Water Depth	fathom	1 fathom	m
Atmospheric Pressure	In. of Hg	.01 in. of Hg	———
Visibility	n. mi.	1 n. mi.	———
Cloud Cover	%	10%	———
Cloud Type	Cu, Ci, etc.	———	———
Precipitation	(Yes or No)	———	———
Forel-Ule Color	Comparator Unit	———	———
Chlorophyll		.1 mg/m^3 (lab analysis)	———

Table 4. Fisheries Parameter Requirements

PARAMETER	METHOD	UNIT
Species I. D.	Observation	Common Name
	Port Sampler	Common Name
Time Fish Hooked	Observation	Local Time Hour/Min.
Time Fish Raised	Observation	Local Time Hour/Min.
Time Fish Lost	Observation	Local Time Hour/Min.
Time Fish Boated	Observation	Local Time Hour/Min.
Bait	Observation	Common Name
Water Color	Observation	Color Description
Surface Conditions (Grass, Rips, Etc.)	Observation	Description
Location of Fishing	Loran	Square
	Dead Rec/Compass	Square
Fishing Time Start	Observation	Local Time Hour/Min.
Fishing Time End	Observation	Local Time Hour/Min.
No. Rods Fished	Observation	Number
Bait Fished	Observation	Common Name
Billfish Girth	Measurement	Cm
Billfish Sex	Observation	
Billfish Weight	Measurement	Pounds
Billfish Length		
Lower Jaw to Fork	Measurement	Cm
Orbit to Fork	Measurement	Cm
Gamefish No. Caught	Count	Number
Gamefish Time Caught	Observation	Local Time Hour/Min.
Boat Captain/Owner	Registration	
Boat Name	Registration	

SECTION 5

FIELD OPERATIONS AND DATA ACQUISITION

5.1 STRATEGY

The incidence of gamefish in the northeastern Gulf of Mexico dictated that operations be conducted during June-September. Operations were limited by resources to no more than two separate periods which had to be scheduled for weekends in order to obtain maximum participation by sportsfishermen and the five day repeating ground track Skylab overpass limited the number of weekends available. Of those overpasses occurring on weekends a number were considered unsuitable for remote sensing because of the low sun elevation angle at the time of overpass. Based on these considerations, field operations were scheduled for 1 through 3 June and 4 and 5 August. Selection of the latter period was influenced also by concern that the EREP mission of Skylab 3 might be terminated early.

The June mission proved nonproductive relative to data acquisition because Skylab EREP was reassigned due to adverse weather forecasts, the earth survey aircraft overflight was cancelled and the fish catch was extremely low. The meager data sets precluded worthwhile analysis, therefore no further discussion of the June data acquisition is presented in this text.

Contingency plans with different data acquisition transects were issued in a field operating plan (14) for the 4 and 5 August mission to permit adjustments in aircraft and surface data acquisition as required by fishing and oceanographic conditions and the Skylab EREP overpass. Acquisition coverage could be shifted spatially and temporally by appropriate selection of the plans. In order to provide a basis for selection, a pre-operational sampling was taken. The NOAA Research Vessels Oregon II and George M. Bowers entered the test site on 3 August, obtained oceanographic measurements and radioed the information to the Principal Investigator at the Destin Information Center. In addition, local fishermen were canvassed relative to fishing conditions. Imagery from weather satellites was obtained and accorded quick look evaluation for environmental information. The flight lines and surface transects selected on the basis of this pre-operational evaluation and used during 4 and 5 August operations are shown in Figures 7 and 8. Sea truth sampling station coordinates for the oceanographic vessels are listed in Table 5.

5.2 MANAGEMENT

A committee of representatives from six gamefishing clubs and charterboat associations headquartered in Alabama, Florida, and Louisiana, coordinated the volunteer fishing program to acquire data on the living marine resource. These data were acquired through a Skylab Gamefish Tournament held 4 and 5 August under the general management of the Pensacola Big Game Fishing Club.

Management information centers were activated two weeks in advance of field operations in office trailers at three check point marinas in Pensacola, Destin and Panama City, FL.

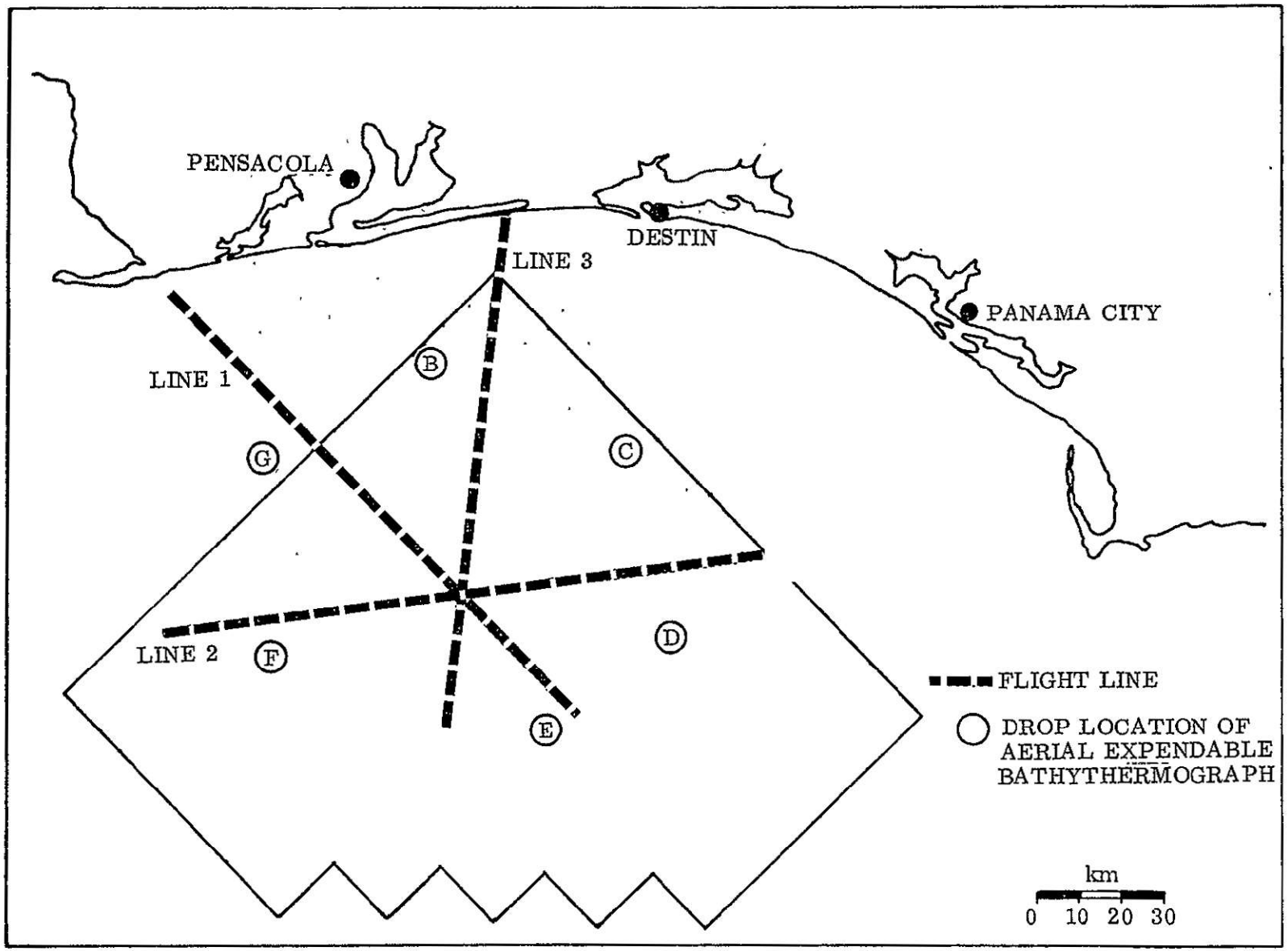

Figure 7. Aircraft Transects - 4-5 August

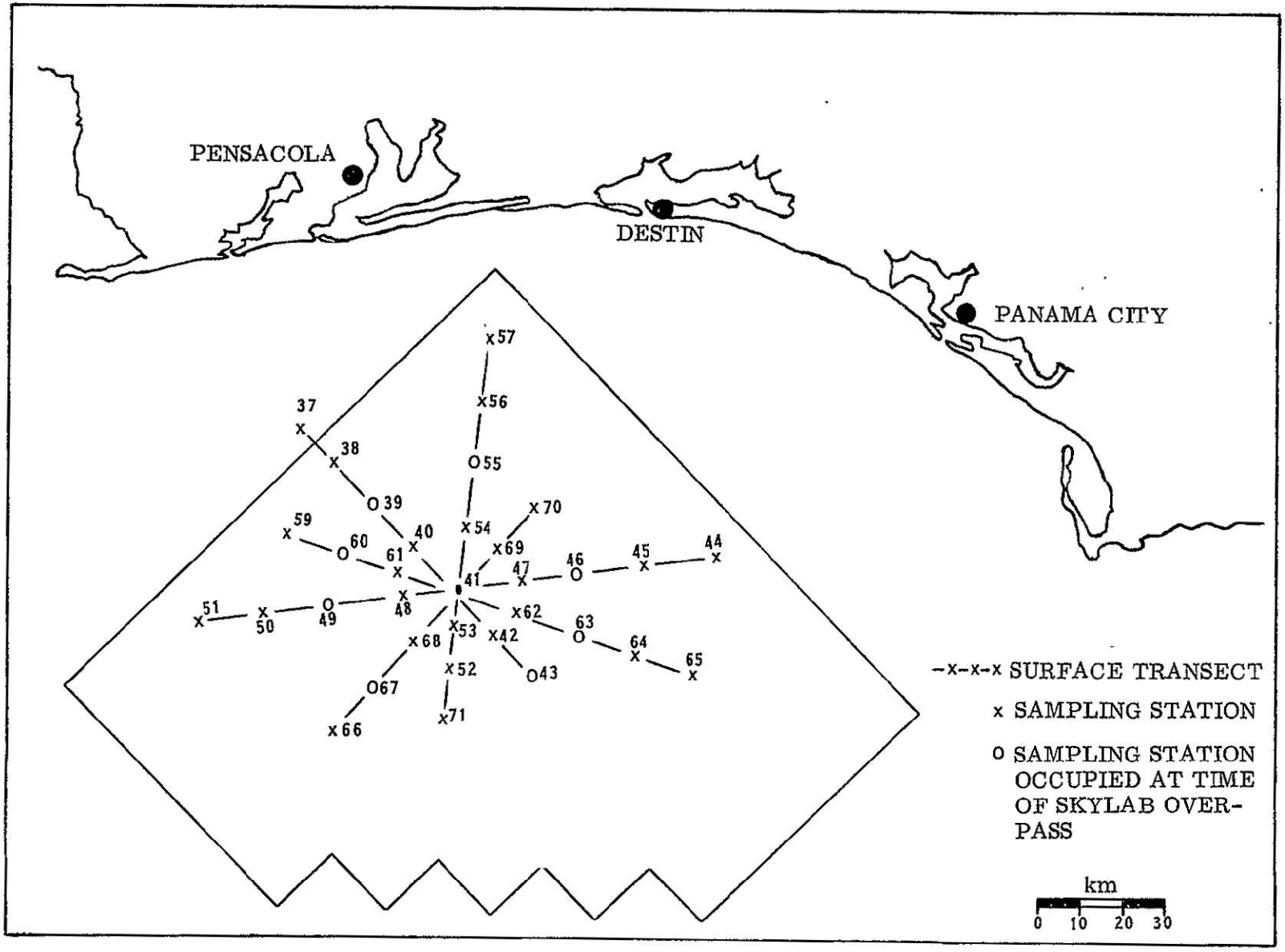

Figure 8. Surface Transects and Oceanographic Sampling Stations, 4 and 5 August

Table 5. Sea Truth Sampling Station Coordinates for Oceanographic Vessels

STATION NUMBER	BOAT		LATITUDE	LONGITUDE
37	# 6	MARIC IV	29°58.0'N	87°21.5'W
38	6		29°52.0'N	87°15.5'W
39	6		29°46.2'N	87°09.5'W
40	6		29°40.3'N	87°03.2'W
41	# 1	ERL	29°34.5'N	86°56.75'W
42	# 4	OREGON II	29°28.6'N	86°51.0'W
43	4		29°23.5'N	86°45.5'W
52	4		29°24.0'N	86°58.25'W
53	4		29°30.0'N	86°57.5'W
71	4		29°17.5'N	86°59.0'W
57	# 3	RACHEL	30°07.0'N	86°52.5'W
56	3		29°58.75'N	86°53.75'W
55	3		25°51.0'N	86°54.75'W
54	3		29°42.5'N	86°55.75'W
44	# 2	NO HU HU	29°39.5'N	86°17.0'W
45	2		29°38.25'N	86°27.4'W
46	2		29°37.0'N	86°37.0'W
47	2		29°35.5'N	86°47.0'W
51	# 5	CAP'N DUSTIN	29°29.0'N	87°36.5'W
50	5		29°30.5'N	87°26.5'W
49	5	AND GLORY	29°31.7'N	87°16.5'W
48	5		29°32.75'N	87°06.5'W
58	# 7	GULFSTREAM	29°45.0'N	87°32.5'W
59	7		29°42.5'N	87°23.5'W
60	7		29°39.8'N	87°14.5'W
61	7		29°37.0'N	87°05.5'W
65	# 8	KINGFISH II	29°23.0'N	86°20.5'W
64	8		29°26.0'N	86°29.3'W
63	8		29°28.7'N	86°38.5'W
62	8		29°31.5'N	86°47.5'W
70	# 9	GEORGE M.	29°45.9'N	86°44.5'W
69	9	BOWERS	29°40.2'N	86°50.7'W
68	9		29°28.3'N	87°03.5'W
67	9		29°22.3'N	87°10.0'W
66	9		29°16.5'N	87°16.5'W

The primary purpose of the early activities was to solicit local angler participation and to provide a contact for local anglers requiring tournament information. The coordinators, manning the centers, accepted additional tournament entries for forwarding to the Pensacola Big Game Fishing Club; provided invitational packages to prospective tournament participants; made cooperative arrangements for scientific observers to board gamefishing boats; provided experiment information to tournament participants; and served as local communication outlets on project matters. NMFS and NASA management personnel moved to the information centers from the NSTL on 3 August. During 4 and 5 August assigned personnel (14) supported the data acquisition programs, supervised port sampling, maintained fish catch records, collected oceanographic data load forms, monitored tournament boards, and monitored activities at respective check points.

The Principal Investigator established a control center for the field operation at the Destin Information Center because of its centralized geographic location. A temporary radio station was set up by NASA at this center and maintained direct communications with the aircraft during overflights. The NASA vessel, ERL, while on station at the hub of surface operations served as a communications relay between the control center and the surface vessels. In order to facilitate management decisions during operations, the control center was equipped with a series of operational charts (Table 6) for information display, grease pencil recording of data, and quick look analysis.

5.3 SKYLAB EREP

The Skylab EREP overpass occurred on track 62 at approximately 1140 CDT on 5 August with 40 to 70 percent cumulus cloud cover. Duration of the overpass was about 40 seconds as the satellite transited southeasterly over the test site from the direction of Mobile Bay. The sensors activated during the overpass are shown with their planned applications for the project in Table 7. Actual application is shown in Appendix B.

NOAA-2 and USAF DAPS overpasses also occurred during the operation as indicated in Table 7. DAPS imagery was received prior to operations and was useful in forecasting operational conditions.

5.4 AIRCRAFT

Three aircraft flew data gathering missions on the morning of 5 August. A NASA earth survey aircraft, the NC130B, based in Houston, TX, and a local NASA contracted aircraft, the E-18, each flew three flight lines (Figure 8) at altitudes of 6100 m and 3000 m respectively. Each set of flight lines totaled 413 km. The NC130B reported cloud cover of less than 10 percent at completion of the first flight line at 0900 but weather conditions deteriorated during the day. The third aircraft, a Navy NP3A operating out of Jacksonville, FL, dropped expendable bathythermographs for data to be used in a separate study. Aircraft sensor coverage appears in Table 8 with actual application as shown in Appendix B.

The NASA aircraft had originally been scheduled to overfly the test site at the time of the Skylab overpass on 5 August but the flight lines were flown several hours earlier due to concern about the weather. The E-18 was also scheduled for a flight on 4 August but the flight was cancelled due to adverse weather conditions.

Table 6. Status Display Charts

	General Information Charts
GI-1	Oceanic/Gamefish Project Objectives
GI-2	Participating Agencies
GI-3	Project Schedule
GI-4	Project Results
	Weather Information Charts
WI-1	Current Local Weather
WI-2	Current Local Weather Map
WI-3	Current Local Weather Charts (Use oceanographic chart 1 each August 4 and 5)
	Oceanographic Information Charts
OI-1	Oceanographic Sea Truth Observations (1 set August 4 and 1 set August 5)
OI-2	Oceanographic Station Chart Plan A (Big Charts) Plan B Plan C Plan D
OI-3A	Sea Surface Temperature Chart (Overlay for each day, August 4 and 5)
OI-3B	Sea Color Chart (Overlay for each day, August 4 and 5)
OI-3C	Secchi Disc Chart (Overlay for each day, August 4 and 5)
OI-4	Preliminary Oceanographic Chart (3 overlays - Temperature, Color, Secchi, Full size # 1115 chart)
OI-5	Oceanographic/Fishing Data Chart (1 per day August 4 and 5)

	Biological Information Charts
BI-1	Biological Data
BI-2	Biological Data Acquisition (1 chart each August 4 and 5)
BI-3	Biological Data Coverage (Blank fishing chart 1 each August 4 and 5)
BI-4	Skylab/Gamefish Tournament Scoreboard
	Space Information Charts
SI-1	Skylab Pass Schedule/Status
SI-2	Skylab Instrument Coverage/Status
SI-3	Skylab Track Chart
SI-4	C130 Pass Schedule Track/Status (2 sets, 1 each August 4 and 5)
SI-5	C130 Instrument Coverage/Status (2 sets, 1 each August 4 and 5)
SI-6	C130 Track Chart
SI-7	E18 (Beechcraft) Pass Schedule/Status
SI-8	E18 Instrument Coverage/Status
SI-9	E18 Track Chart (3 sets August 4, 5, and 10)
SI-10	NP3A Navy Recon. Pass Schedule/Status (AXBT overlay and dropsonde)
SI-11	NP3A Instrument Coverage/Status
SI-12	NP3A Track Chart
SI-13	DAPS (USAF Data Acquisition and Processing System/Status)
SI-14	DAPS Instrument Coverage Status
SI-15	DAPS Track Chart

Table 7. Satellite Sensors Activated

INSTRUMENT	DESCRIPTION	FOOTPRINT	USE
		EKYLAB EREP	
S190 A	6 Cameras	163 km wide	Water Color, Surface Features
S190 B	1 Camera	109 km wide	Water Color, Surface Features
S191	Infrared Spectrometer	.43 km wide	Water Color, Sea Surface Temperature
S192	Multispectral Scanner	74 km wide	Water Color, Sea Surface Temperature
S194	Microwave Radiometer	109 km wide (half power)	Sea Surface Salinity
		NOAA-2	
VHRR-IR	Very High Resolution Radiometer, Infrared	-	Sea Surface Temperature
VHRR-VIS	Very High Resolution Radiometer, Visual	-	Sea Surface Temperature
		DAPS	
IR	Infrared Scanner	-	Sea Surface Temperature
Visual	Reflectance Image	-	Surface Features

5.5 SEA TRUTH

Data task teams on four Government and five Government-chartered vessels operating out of Orange Beach, AL, Destin, FL, and Panama City, FL, gathered sea truth environmental data at 48 sampling stations at intervals of one and a half hours during daylight hours on 4 and 5 August. A total of 140 sets of measurements were taken at sampling stations shown along transects in Figure 8.

Parameters measured for each set included surface water temperature, air temperature, Secchi disc extinction depth (as measure of turbidity), sea state, wind direction and speed,

Table 8. Aircraft Sensor Coverage

INSTRUMENT	DESCRIPTION	FOOTPRINT	USE
NASA NC130B			
MSS	Multispectral Scanner	10.2 km	Sea Surface Temperature, Water Color
RECON IV	Infrared Scanner	7.0 km	Sea Surface Temperature
AMPS	Airborne Multispectral Photographic System	2.3 km	Water Color
RC8	Aerial Camera/Color Photography	9.1 km	Cloud Cover, Water Color, Location of Surface Vessels and Features
I^2S	Multiband Camera	5.3 km	Water Color
PRT 5	Precision Radiation	0.2 km	Sea Surface Temperature
NASA Light Aircraft			
RS-18	Thermal Infrared Scanner	7.3 km	Sea Surface Temperature
K-17	Aerial Camera/Color Photography	4.8 km	Water Color, Surface Features
EL 500	2 Cameras - Color and Color IR	4.2 km	Water Color, Surface Features
PRT 5	Precision Radiation Thermometer	0.1 km	Sea Surface Temperature
E 20-D	Spectrometer	0.1 km	Water Color

wet and dry bulb temperature, water depth, atmospheric pressure, visibility, cloud cover and type, and water color. Sea water samples were also taken for laboratory analysis of salinity and chlorophyll-a, -b, and -c. The Forel-Ule color comparator was used to determine water color, and sea surface temperature was obtained by means of a bucket thermometer. In addition, portable salinometers were used on several vessels to obtain in situ salinity and temperature measurements. Relative irradiance readings were taken at the hub station (Station 41) and spectroradiometer data was collected on two vessels but the measurements were not used in the analyses reported in this text.

In addition to data acquisition by the oceanographic vessels, a total of 75 sets of measurements coincident with gamefish catches were collected by scientific observers aboard 12 gamefish boats. The parameters measured by these observers were the same as those measured from the oceanographic boats except that chlorophyll samples were not taken. Pyschrometer readings were taken on only a few boats.

5.6 GAMEFISH DATA

Sportsfishing boats were generally underway at first light in order to reach favorite fishing areas in time to commence trolling at the tournament start-up time of 0900 CDT. The favorite area for many anglers was the central and south central portion of the test site. The eastern and western portions were largely unfished. These and other preferences resulted in a highly uneven distribution of fishing pressure on both tournament days. Assignment of boats to fishing squares in order to equalize fishing pressure was considered in operational planning but was discarded as unacceptable from the anglers' viewpoint.

A number of boats remained out in the area overnight. Because of the fuel shortages and the long trip in and out, it had been anticipated that a few boats would choose this course of action. The NOAA R/V Oregon II remained near the center of the fishing area during the night to take gamefish aboard for cold storage as requested. Several boats took advantage of this option.

From mid afternoon through evening twilight on each day of the tournament, returning boats, often in traffic jams at the check points, docked briefly for data submission to the port samplers and the tournament weighmasters' attentions relative to their catch. A few boats were unable to make the check points and data was either phoned or mailed in by boat owners and captains. Submission of the Gamefish Boat Log data format (Appendix A) was the indicator of tournament participation. The numbers of boats participating in the tournament by check point are listed in Table 9. As many as 325 anglers participated in the tournament.

Table 9. Boat Participation in Tournament

Date	Pensacola	Destin	Panama City	Total
4 August	26	50	6	82
5 August	24	39	6	69

Activities were particularly rushed on the afternoon of 5 August. A number of boats that had not reported in on 4 August reported in on 5 August with two days results. As many as six white marlin lay on the landing at Destin at one time as the weighmaster processed them through weigh-in. Three port samplers were simultaneously interviewing boat captains, obtaining catch measurements and completing the boat logs while other personnel contacted anglers for data source information.

Other project personnel provided tournament patches and boat decals to boat captains and anglers as they were debriefing. Boat traffic along the dockside was heavy at times with several boats lining up for approaches while others were casting off. Four boats may be seen in Figure 10 clustered around the east end of the Destin check point landing.

Boat captains recorded all fish raised but not hooked, hooked, lost, and boated. Information was also recorded on the number of fishing lines used, the interval that lines were in the water, bait used and any water anomalies observed whenever fish were caught. At the time

of submission, each log was reviewed by a port sampler with the respective boat captain for omissions and errors. Table 10 gives a catch breakdown of the seven tournament species as reported by boat logs. Catches of white marlin and dolphin far exceeded that of other species. Photographs of the two species are shown in Figures 9 and 10.

Table 10. Tournament Fish Catch, 4 and 5 August

Fish Species	No. Raised But Not Hooked		No. Hooked		No. Lost		No. Boated	
	4 Aug.	5 Aug.	4 Aug.	5 Aug.	4 Aug.	5 Aug.	4 Aug.	5 Aug.
BILLFISH								
Blue Marlin	5	3	6	5	6	5	0	0
White Marlin	25	19	32	23	9	14	23	9
Sailfish	4	5	10	4	6	3	4	1
Total Each Day	34	27	48	32	21	22	27	10
OTHER GAMEFISH								
Yellowfin Tuna	0	0	0	0	0	0	0	0
Bluefin Tuna	0	0	0	0	0	0	0	0
Dolphin	2	0	32	43	5	5	27	38
Wahoo	4	0	10	6	2	3	8	3
Total Each Day	6	0	42	49	7	8	35	41
ALL TOURNAMENT GAMEFISH								
Total Each Day	40	27	90	81	28	30	62	51
Tournament Totals	67		171		58		113	

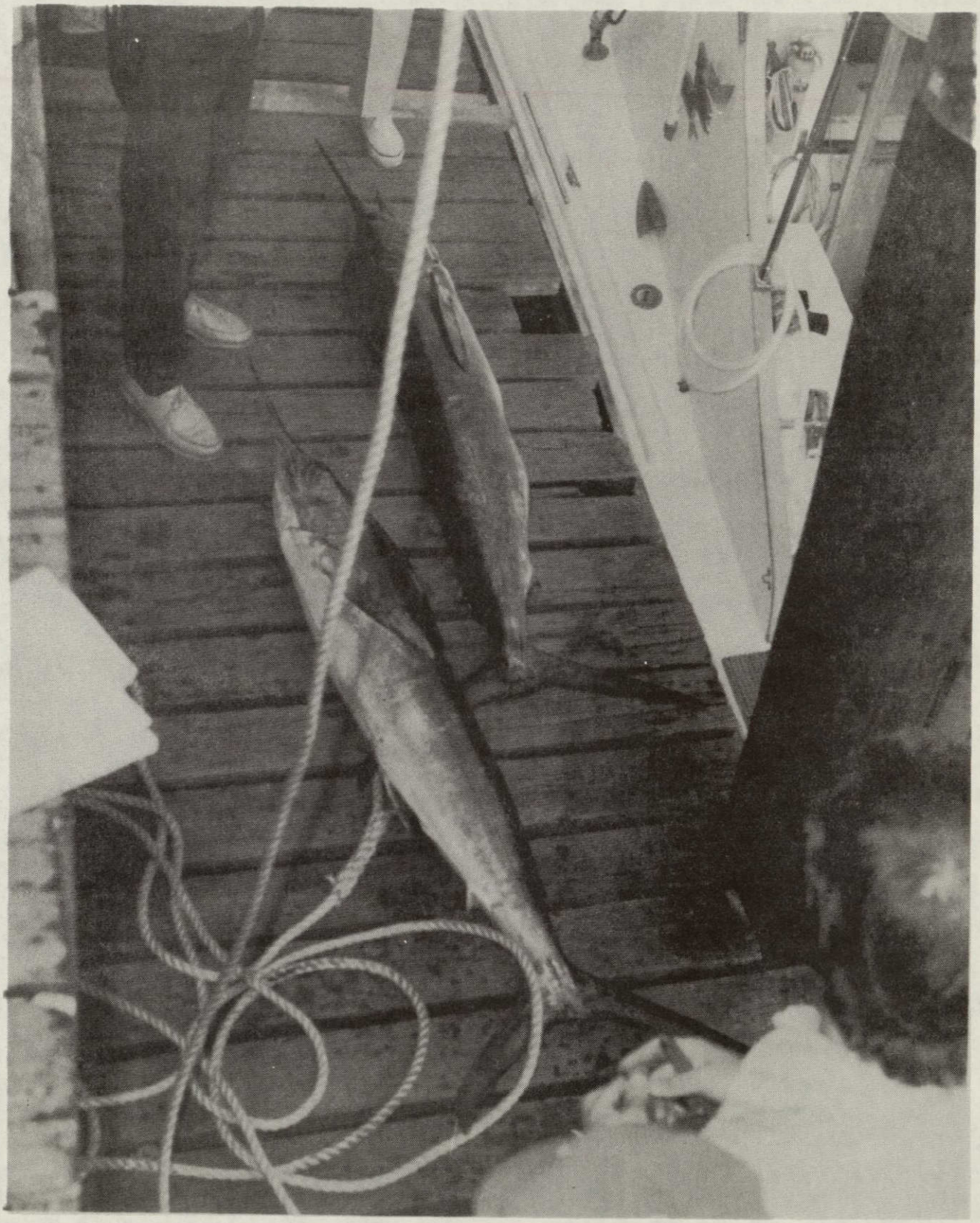

Figure 9. White Marlin at Destin Check Point

Figure 10. Dolphin Weigh-In

SECTION 6

DATA ANALYSIS

6.1 GENERAL

The primary objective of the investigation was to establish the feasibility of using remotely sensed data, acquired by satellite and aircraft, to determine the availability and distribution of oceanic gamefish. The sensors used in this investigation did not have the capability for direct observation of the gamefish and had only limited capability for acquisition of information related to surface or near surface phenomena. Therefore, the main thrust of analysis utilized an indirect approach with intermediate correlations. The resource data and remotely sensed information were separately related to the sea environment as observed by surface sampling and through the latter related to each other (Figure 11). Emphasis was placed on the direct relationship between the remotely sensed surface phenomena and the incidence of gamefish during the latter stages of the analysis. The analysis associated with both the direct and indirect phases of the approach is discussed in the remaining sections of the report.

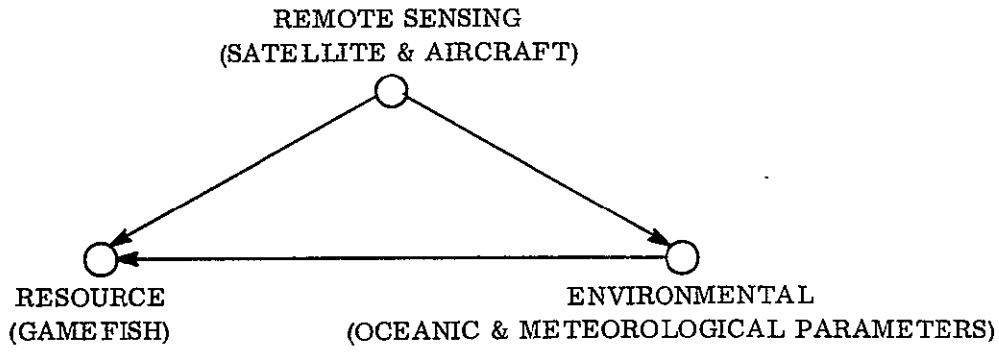

Figure 11. Analysis Approach

The final product of the analysis was envisioned as a prediction model using remotely sensed data or oceanographic values inferred from remotely sensed data for resource utilization. During the application of the approach the following assumptions were tested.

- Data acquired with satellite and aircraft remote sensors can be used to predict fish distribution and availability.
- There exists a cause/effect relationship between selected oceanic conditions and the distribution of gamefish stocks.
- Oceanographic information can be used to assist recreational fishermen in their activities.

Preliminary results (15) of data analysis were presented on 17 April 1974 at the Ninth International Symposium on Remote Sensing of Environment, Willow Run, Michigan. The feasibility of utilizing remotely sensed data to assess and monitor oceanic gamefish (16) was presented at the Earth Resources Survey Symposium, Houston, Texas in June 1975.

6.2 RESOURCE AND SEA TRUTH RELATIONSHIPS

6.2.1 CONCEPT

The concept employed in the analysis was that oceanic gamefish abundance and distribution can be expressed as a function of the environment, which is similar to that concept expressed in a previous fisheries remote sensing paper (17). The functional dependence is described in the following algebraic expressions.

$$A_{x,y} = f(E)$$

$$D_{x,y} = g(E)$$

where:

A = number of oceanic gamefish
x,y = fish location coordinates
E = environmental conditions at x,y
D = gamefish distribution parameters

$$D = \begin{cases} 0 & \text{no fish present} \\ 1 & \text{fish present} \end{cases}$$

The abundance parameter, $A_{x,y}$, was estimated by oceanic gamefish raised only, hooked, lost, or boated by the fishermen and therefore has a larger degree of error due to the ability of anglers to identify, attract, hook and land the fish. The distribution parameter, $D_{x,y}$, by its definition was less susceptible to error than the abundance parameter, $A_{x,y}$, and therefore was utilized in the mathematical modeling efforts.

6.2.2 DATA PREPARATION AND RESOURCE SPECIES SELECTION

Resource information was available for only 34 of the 54 fishing squares on 4 August and 30 of the 54 squares on 5 August. However, environmental information was not obtained from some squares for which there were catch data. Accordingly, an averaging technique was used to provide environmental information for those squares where resource data had been recorded. The technique consisted of averaging the values of all encircling squares and had previously been used for interpolating catch data (18). Furthermore, individual test square values for each parameter were computed by averaging all station readings in that square for each day. Environmental data for each square fished consisted of the following parameters: Surface water temperature, surface salinity, air temperature, Secchi extinction depth, sea state, Forel-Ule water color, chlorophyll-a, chlorophyll-b, chlorophyll-c, water depth, and distance from shore. These parameters were utilized as independent variables in the initial correlation analyses. Atmospheric pressure was eliminated from the analyses because of the limited number of stations for which this measurement was reported.

Initially it was decided to concentrate efforts on a billfish and a non-billfish species. White marlin and dolphin respectively were selected because a relatively large catch data set was available for each. As planned, subsequent to the white marlin analysis, correlations were investigated for 4 and 5 August and the combined dates between dolphin distribution and abundance and the environmental parameters - sea surface temperature, salinity, air temperature, Secchi extinction depth, sea state, Forel-Ule color, water density and chlorophyll-a, -b, and -c. Instability was found to exist for all relationships on a day to day comparison. The extent of the instability discouraged development and testing of prediction distribution and abundance models for dolphin such as were accomplished for white marlin. The white marlin was selected because interest seemed to focus on billfish and accordingly, much of the text on the progress of the analyses relates to white marlin.

The white marlin is one of the more dramatic big game/deep water sportsfishes. It occupies a home range comprising a great portion of the Atlantic Ocean and the Gulf of Mexico. While the fish does not reach as large a size as other spearfishes, it is by no means second-rate in looks, biology, and popularity.

Named from a shortened form of "marline spike," a pointed nautical device used to separate strands of rope while splicing, the species generally shows more green than most marlins. Its upper body is a brilliant greenish-blue, but coloration changes abruptly to silvery white at about the level of the lateral line. Light blue vertical bars run the length of the fish, but they quickly fade and eventually disappear soon after the fish dies.

Of all the marine species, the white marlin, according to Dr. Maurice Burton, International Wildlife Institute, is believed to be the fastest fish in the water. It can reach speeds of up to 50 miles per hour because of its "streamlining." When pursuing a meal at top speed, all its fins except the tail fin are folded down into grooves in its body so that no bothersome obstructions prohibit easy passage of water across its shape. Additionally, its long beak forms a highly effective cutwater.

Marine biologists believe that the white marlin follows set migratory patterns regulated solely by food availability. In the past, white marlin catches in the Gulf of Mexico made headlines, but that happens no longer. With each passing summer, July through October being prime months, large catches make for fine offshore sportsfishing.

White marlin first were discovered in the gulf in the mid-50's when the U. S. Fish and Wildlife Service began to explore angling potential along the 100-fathom curve which comes close to South Pass below New Orleans. The species is caught both in bluewater and greenwater offshore.

Like its relatives (sailfish and broadbill swordfish), the white marlin uses its spear to cripple or kill its prey. Favorite foods include herring and squid, but it also will eat practically anything it can capture, especially anchovies and jacks.

This dietary versatility makes fishing for white marlin, where bait is concerned, an easy matter. The most popular natural baits are small mackerel, bonito, herring, mullets, and other small but elongated species. As well as natural baits, the fish will strike almost any kind of artificial lure from spoons to feathers to plugs to jigs.

Anglers prefer the female to the male in the white marlin species since females consistently are larger than the males. Deepwater enthusiasts who fish for whites regularly use tackle ranging from 50-pound test to 125-pound test.

The big fish strikes hard, runs fast, makes repetitive jumps, and can tailwalk in a strong surge almost 100 feet across the surface of the water. Depending upon which technique works best on which day, the preferred method-trolling-for white marlin is to skip the bait behind the boat, either at a normal swimming pace or so fast it barely skims the surface chop. Strikes also are produced when the bait is allowed to drift behind the wake, then gathered in slowly to imitate an injured fish. Because its pelvic fins are far forward and on level with its pectoral fins, the white marlin can turn suddenly in a tight circle to strike a bait more than just once. Most species taken on rod and reel average about 50 to 60 pounds. Maximum recorded weight for the white marlin on sportsfishing tackle is 161 pounds. The first prize winner taken during the experiment weighed 70.5 pounds.

6.2.3 CORRELATION ANALYSIS

Initial correlation analyses were made to determine which form of the resource abundance and distribution parameters (fish raished only, hooked, raised plus hooked, or boated) should be used. The hooked parameter was selected to maximize sample size and minimize error. There was less error in this measurement as compared to the raised parameter, i.e., there is less chance of incorrect identification once the fish is hooked. Conversely, the boated parameter, which had no possibility of identification error, caused a significant error in the distribution parameter, $D_{x,y}$, when the fish was hooked and not boated. Therefore, the hooked form of the parameter was used in correlation analyses and mathematical modeling.

Further error was identified in the resource distribution parameter in that a certain level of fishing pressure was required to determine if there were fish in a fishing square. For example, if fishing pressure was insufficient in a square with environmental characteristics conducive to fish and in one with environmental characteristics not conducive to fish, both would have a value of 0 for the distribution parameter regardless of the presence of fish. This would tend to conceal relationship between the resource and environment. Having found that no white marlin were caught in any of the test squares with less than 4 boat hours of fishing pressure, a correction for this error was made by eliminating from the analyses all squares having less than 4 boat hours of fishing pressure. This resulted in narrowing the study to 24 of the 34 test squares remaining for 4 August, and 22 of the 30 remaining for 5 August.

Correlation and regression techniques were utilized to define relationships between the resource and the environment as defined by sea truth measurements. The number of white marlin hooked in each test square was utilized as a measure of abundance ($A_{x,y}$) and converted to form the distribution parameter ($D_{x,y}$). Linear correlation coefficients were computed for white marlin abundance and distribution and each of the environmental parameters (Table 11) measured on 4-5 August. The results listed in Table 11 show a difference between abundance and distribution and probably reflect error in the abundance parameter. The dubious quality of the abundance parameter led to emphasis on the distribution parameter in the modeling efforts. It should be stressed here that the correlation coefficients are a measure of the linear relationships between the given dependent variables and each environmental parameter respectively, and do not necessarily indicate the set of para-

meters which should be used in developing predictive models. This is due to the fact that in some cases the parameters listed are also statistically correlated. For example, in the test area, water depth and distance from shore have a correlation coefficient of .832 which is significant at the 99% level. Hence, these two parameters are not statistically independent and one or possibly both (depending on interrelation with other parameters) may not be selected as a model parameter. However, the correlation coefficients listed in Table 11 provide a measure of the linear relationship (within this set of data) between the white marlin parameters and each of the environmental parameters.

Assignment of biological significance to these correlations was not within the scope of this study. The parameters measured may only be serving as indices of unmeasured parameters. However, a literature investigation has shown that other investigators (19) have also found temperature to be related to fish distribution. In analyses of the distribution of white marlin Gibbs (19) found that successful white marlin longline sets were made in surface wat temperatures above 24°C. Since the fishing data were collected in August when the Gulf is nearly uniform in surface temperature, 29°C (20), the large catch of white marlin was not unexpected. A factor which should be noted here is that there was a correlation coefficient

Table 11. Correlation Between White Marlin (Hooked) Abundance ($A_{x,y}$) and Distribution ($D_{x,y}$) Estimates and Sampled Environmental Parameters (E)

Parameter	Degrees of Freedom	Correlation Coefficient (r)	
		Distribution	Abundance
Water Temperature (°C)	44	.407***	.310**
Salinity (ppt)	44	-.145	.001
Air Temperature (°C)	44	.113	.218*
Secchi Transparency (m)	44	.129	.269**
Sea State (m)	44	.272**	.183
Forel-Ule Color (units)	44	-.180	-.044
Chlorophyll-a (mg/m^3)	44	.200*	.054
Chlorophyll-b (mg/m^3)	44	.056	-.005
Chlorophyll-c (mg/m^3)	44	.214*	.241*
Water Depth (m)	44	.329**	.170
Distance from Shore (km)	44	.454***	.323**

* 90% significance level ** 95% significance level *** 99% significance level

.407 significant at the 99% level for white marlin distribution and temperature with all of the sampled temperatures measuring between 28.5°C and 31.6°C. The strong positive correlation held true for data taken on both days as well as the combined data sets.

There is no evidence of correlation of either distribution or abundance with depth of water according to Gibbs (19). Thus, the apparent strong depth correlation listed in Table 11 may be valid only in this particular test area and may be seasonal or coincidental.

Positive correlations (significant at the 90% level) between white marlin distribution and the chlorophyll-a and c (phytoplankton measurements) were found. This may be compared to a white marlin study in the Middle Atlantic Bight where important marlin areas showed distinctly high zooplankton volumes (21). The comparison tends to support the correlation if one assumes that zooplankton abundance is a function of phytoplankton abundance.

6.3 REMOTELY SENSED OCEANOGRAPHIC PARAMETERS AND CORRELATIONS WITH THE ENVIRONMENT

The object of this phase of the experiment was to measure water surface temperature, turbidity, and chlorophyll concentration from aircraft and satellite. Techniques currently under development by the NASA ERL were used for the measurements.

6.3.1 SEA SURFACE TEMPERATURE

The remote measurement of sea surface temperature has been widely studied. Absolute accuracies of 0.5°C are readily obtainable from aircraft measurements using one, or in some cases no ground truth calibration (9) (10) (22) (23).

The aircraft thermal data were taken from 3000 meters with an RS-18 scanning radiometer and a PRT-5 radiometer and also from 6100 meters with another PRT-5 radiometer. These radiometers are sensitive in the 8-14 μm regions of the spectrum. The aircraft thermal data have been processed and a radiometric temperature trace along the flight lines developed (Figure 12). From this trace, the temperature at points between the flight lines was interpolated to provide the basis of the contour map shown in Figure 13. For comparison purposes, the contour map of surface temperature determined by surface measurements and corrected for insolation during the ten-hour period of sampling to a time midway through the remote data acquisition exercise is presented in Figure 14. The time correction was performed by computing the change in temperature averaged over the test area on an hourly basis and adding the appropriate change to readings made at times different from the normalization time. A composite of the thermal data from the two aircraft was made to fill in gaps that occurred at different locations along the flight lines for the two aircraft caused by time-varying cloud cover. There were, however, several locations along the flight lines where clouds caused a total loss of data, and other locations where anomalous temperature measurements may have resulted from severe variations of atmospheric conditions.

Comparison of the surface and remote temperature contour maps shows that, while they are not identical, the same basic trends are present in both maps. There are two likely explanations for the discrepancies. The surface measurements were made by many individuals under different conditions, which could easily result in measurement errors of up to 0.2°C (24). Because of the 0.25°C contour interval, errors of this magnitude would distort the

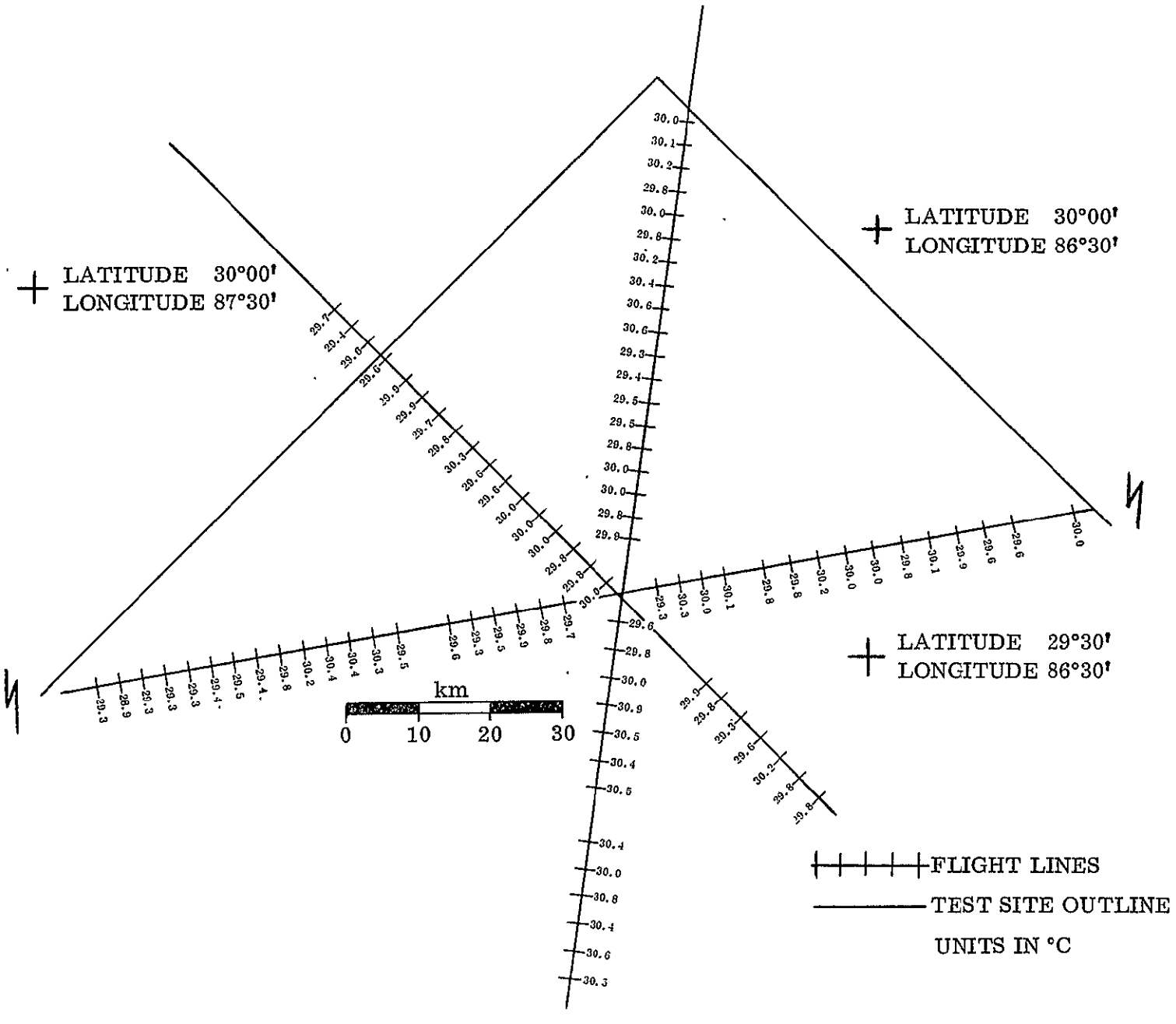

Figure 12. Radiometer Temperature Trace Along Flight Lines

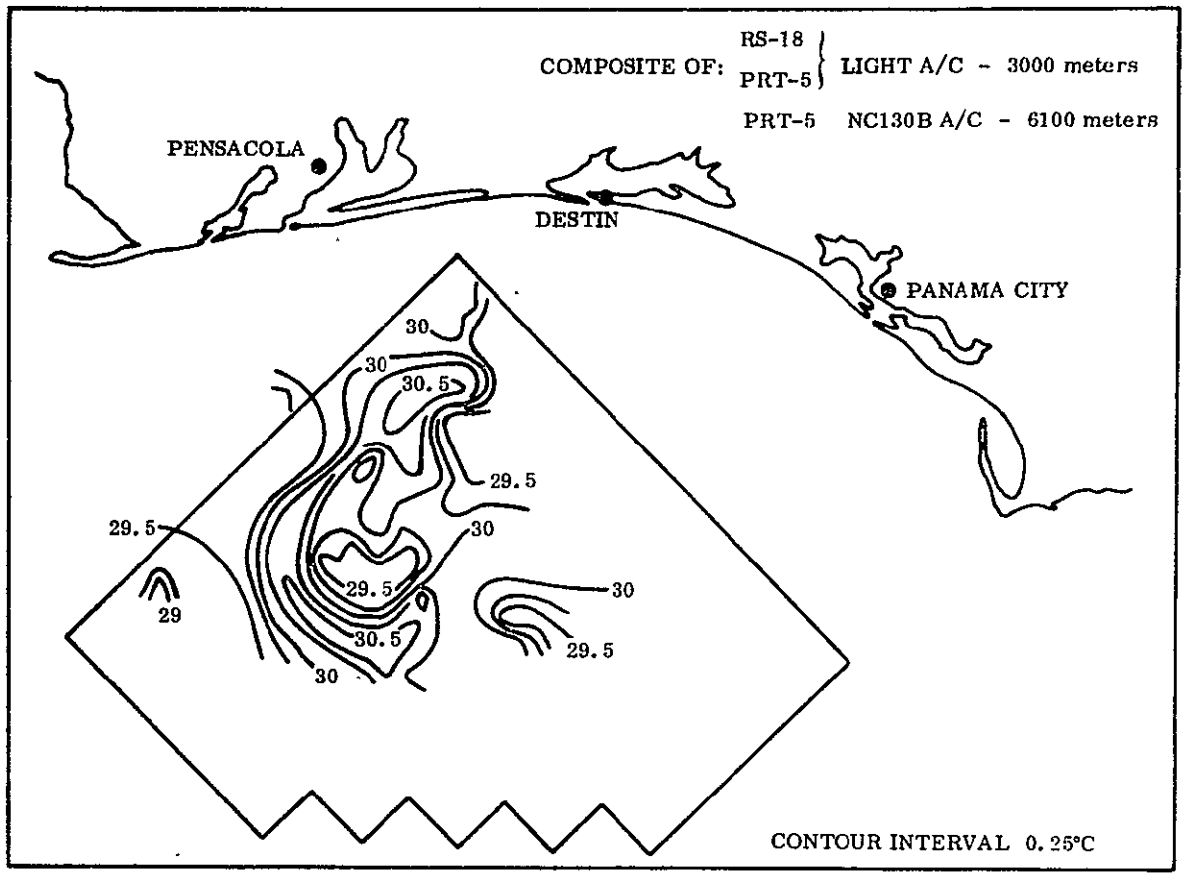

Figure 13. Remote Measurement of Water Temperature

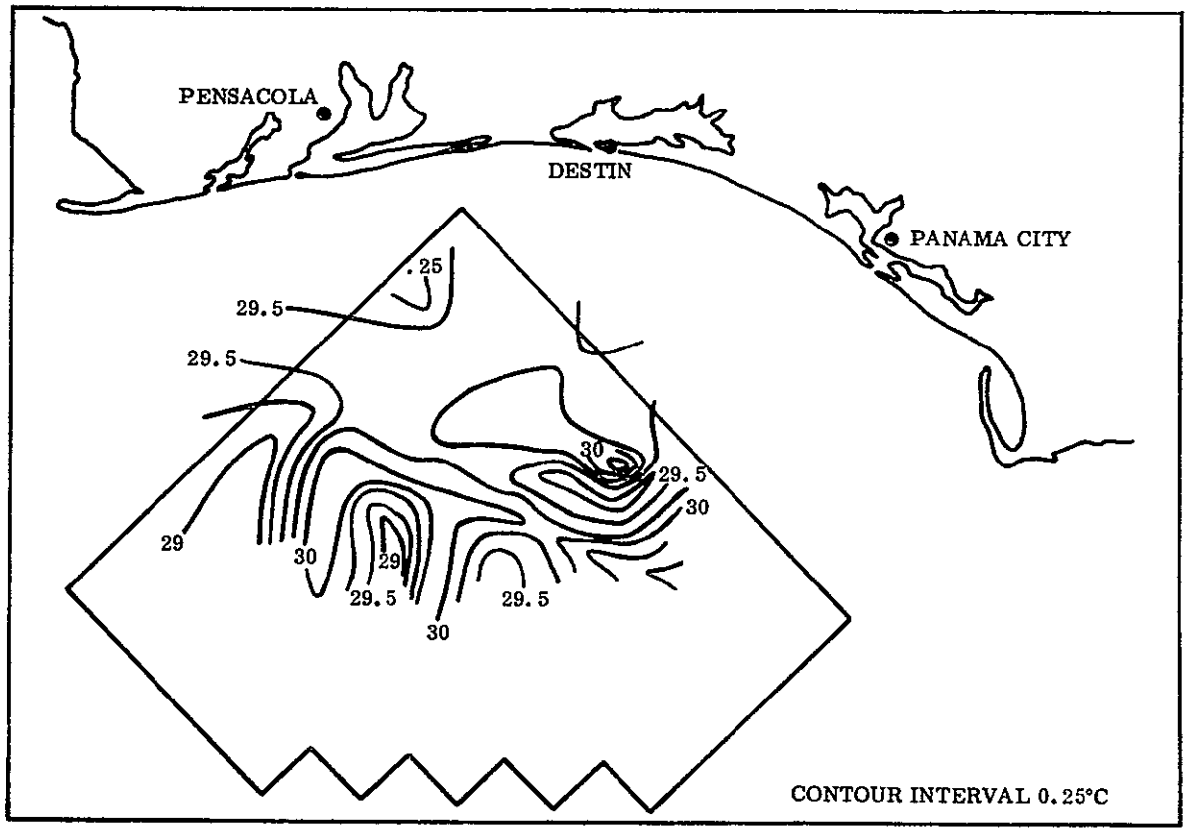

Figure 14. Surface Measurement of Water Temperature

contour patterns. A second explanation is the heterogeneous atmosphere perturbing the remotely measured surface temperature. Analysis of general atmospheric conditions over the test area shows that a variation of 0.23°C can be expected excluding local anamolies due to cloud formations.

It was anticipated that Skylab S192 data would provide thermal measurements over the entire test area. However, analysis of the S192 thermal data revealed it to be unusable for this experiment due to excessive noise.

6.3.2 CHLOROPHYLL

Measurement of chlorophyll-a concentration obtained from radiance measurements has been attempted with varying degrees of success by many workers (12) (25) (26). No technique has apparently achieved either sufficient accuracy or consistency to be generally accepted as the best remote measurement method. The remote data processed in the study were obtained by an Exotech 20-D spectral radiometer, flown on the light aircraft at 3000 meters. The instrument, as configured for this experiment, measured radiance in the region of the spectrum from 390 to 110 nanometers (nm) and calibrated at 57 wavelengths in that range.

An algorithm for computing chlorophyll-a concentration developed by Weldon (12) has been used successfully with data taken with this radiometer, but at lower altitudes over the Mississippi Sound. Weldon's technique consists of a linear function of the difference between the radiance at 620 and 470 nm, normalized by the radiance at 520 nm. The coefficients of the function are determined from ground truth data.

$$C_W = \alpha_1 (R_{620} - R_{470}) / R_{520} + \alpha_2 \qquad \text{(a)}$$

This algorithm was applied to the data acquired in this experiment. The root mean square (rms) deviation of these calculations from the surface measurements was 0.48 mg/m^3 for 18 measurement points, of which nine were used for calibration.

Another technique was used for computing chlorophyll-a concentrations. Examination of the correlation of the 520 nm normalized radiance at each of the 57 wavelengths indicated that the chlorophyll-a concentration was highly correlated with the radiance at 470 and 600 nm. Further analysis showed that a linear combination of these radiance values correlated very well with the square of the chlorophyll-a concentration, so a second calculation of the chlorophyll-a concentration based on spectral radiometer measurements was made using the relation shown in Equation (b).

$$C_c = \sqrt{\alpha_1 (R_{600} - R_{470})/R_{520} + \alpha_2} \qquad \text{(b)}$$

Figures 15 and 16 are the contour maps drawn from the surface and remote measurements of chlorophyll-a, respectively. The remote measurements are a composite (Figure 17) of the results of both calculations. Careful examination of the two sets of measurements showed that the second gave better results in areas where chlorophyll-a content was low, but that the response flattened out at concentrations above 2.3 mg/m^3. The first technique was better at the higher concentrations, so when a concentration greater than 2.0 mg/m^3

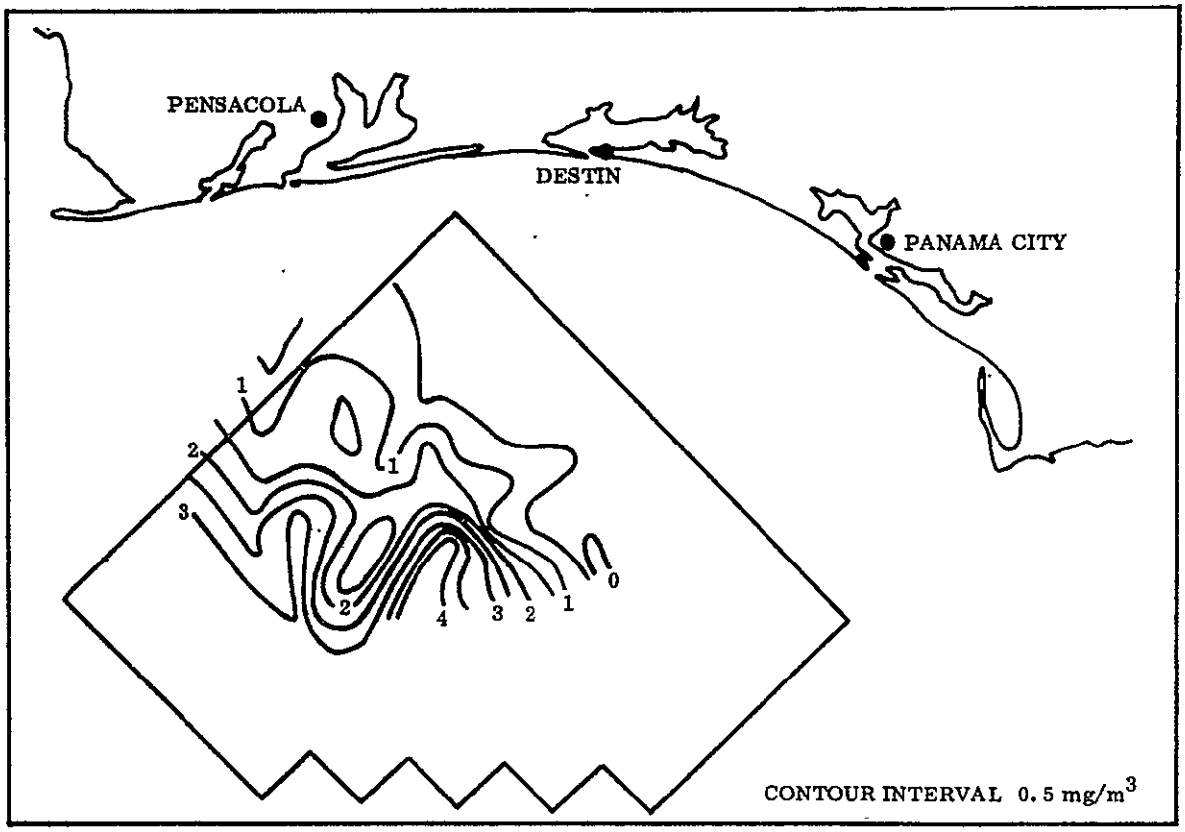

Figure 15. Surface Measurement of Chlorophyll-a

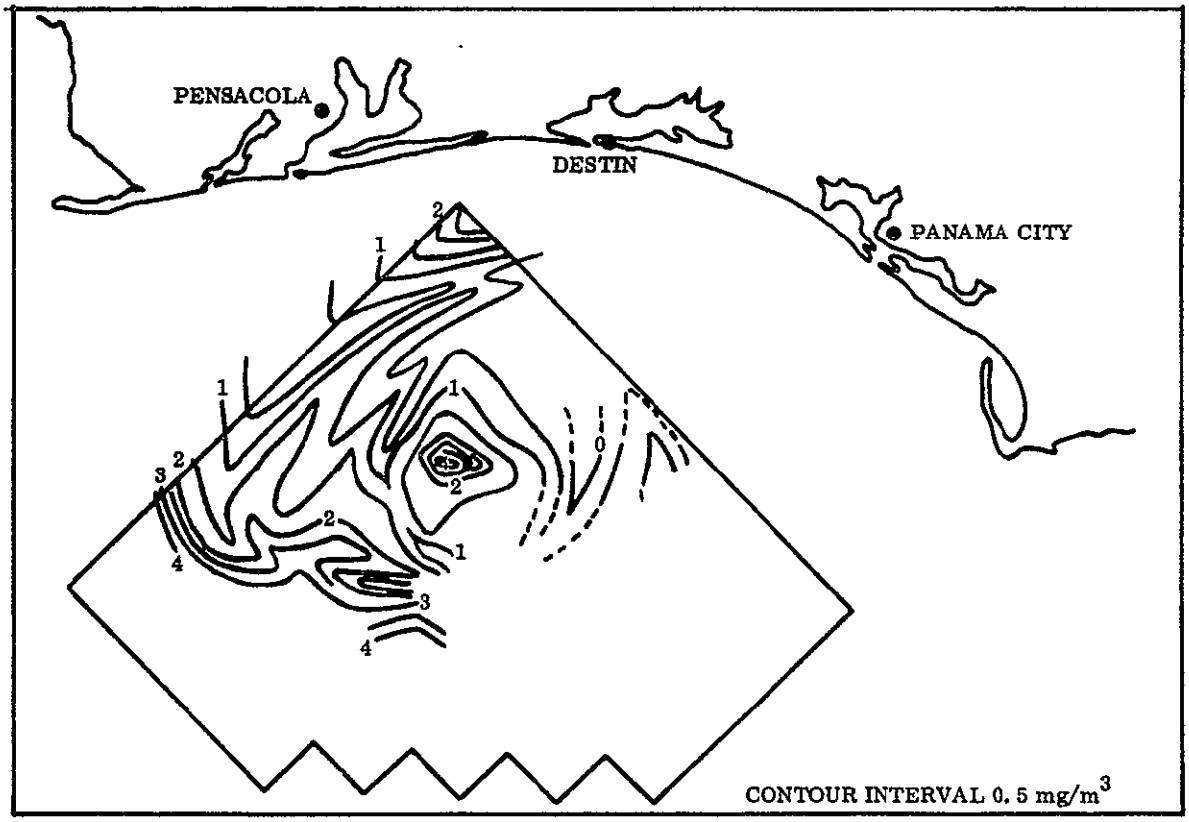

Figure 16. Remote Measurement of Chlorophyll-a

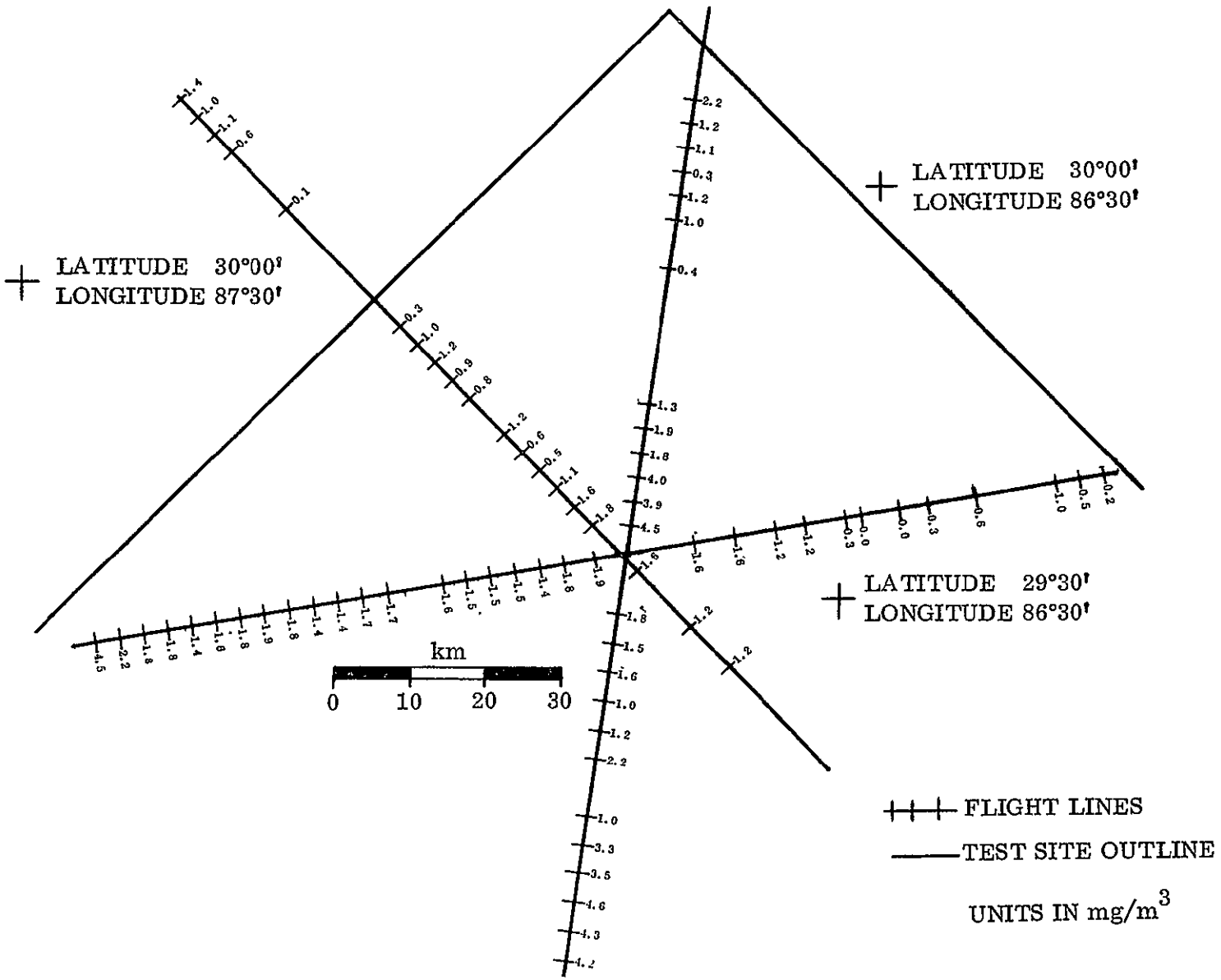

Figure 17. Chlorophyll-a Along Flight Lines

was indicated by the second technique, the value predicted by the first technique was used; otherwise, the value was that computed from Equation (b). The rms deviation of the composite at the 18 surface comparison points was 0.44 mg/m^3.

Comparison of Figures 15 and 16 shows that, while the maps do show significant differences, the large variations present in the surface data are also found in the remote data. This may be readily observed in Figure 18 which is a comparison of chlorophyll-a remote and surface measurement profiles along flight line two. In addition, there are some rapid changes indicated in the remote data which are not seen in the surface data. This does not mean that either measurement is in error; the remote data is a continuous sampling while the surface measurements are separated by approximately an hour's cruise. Another factor to be considered is the 10% repeatability factor (11) of the surface chlorophyll-a determination. It must also be remembered that no corrections for atmospheric conditions were made. These conditions were not constant over the test area, and clouds and cloud shadows do affect the apparent color and hence the inferred chlorophyll-a content.

6.3.3 TURBIDITY

For this experiment, turbidity was measured as Secchi extinction depth. This surface truth measurement of turbidity was used because of operational considerations, i.e., the technique is simple and the necessary equipment inexpensive. However, the measurement is subjective because of the human factor involved and is thus susceptible to considerable error.

Weldon (12) developed an algorithm for computing Secchi extinction depth from spectral radiometer measurements, so the first attempted remote measurement of turbidity was with this technique. Weldon (12) found that the Secchi extinction depth was proportional to the ratio of the radiance measured at 600 nm to that at 550 nm, but application of this algorithm to the data acquired in the gamefish experiment was notably unsuccessful. The failure of this previously verified technique is probably due to the fact that Weldon's work was done with measurements made in the Mississippi Sound where three meters is generally the greatest Secchi depth observed, as opposed to thirty meters in the Gulf. Several techniques were developed to infer turbidity measurements from the spectrometer data.

The final algorithm as in the chlorophyll calculation optimized the information content relative to the Secchi transparency measurement. This optimization was performed by selecting wavelengths which showed the highest correlation with the Secchi depth and the least correlation with each other. Unnormalized radiance data, radiance normalized by a wide band in the blue (390-430 nm) region, and radiance normalized by a wide band in the infrared (911-1073 nm) region were examined. The best set of correlations was found with three wavelengths (410, 440, and 550 nm) of the blue-normalized radiance. An expression of the form

$$S_c = \sum_{n=1}^{3} \alpha_n R_{\lambda_n}/R_{blue} + \alpha_4 \qquad (c)$$

was used to calculate the Secchi extinction depth.

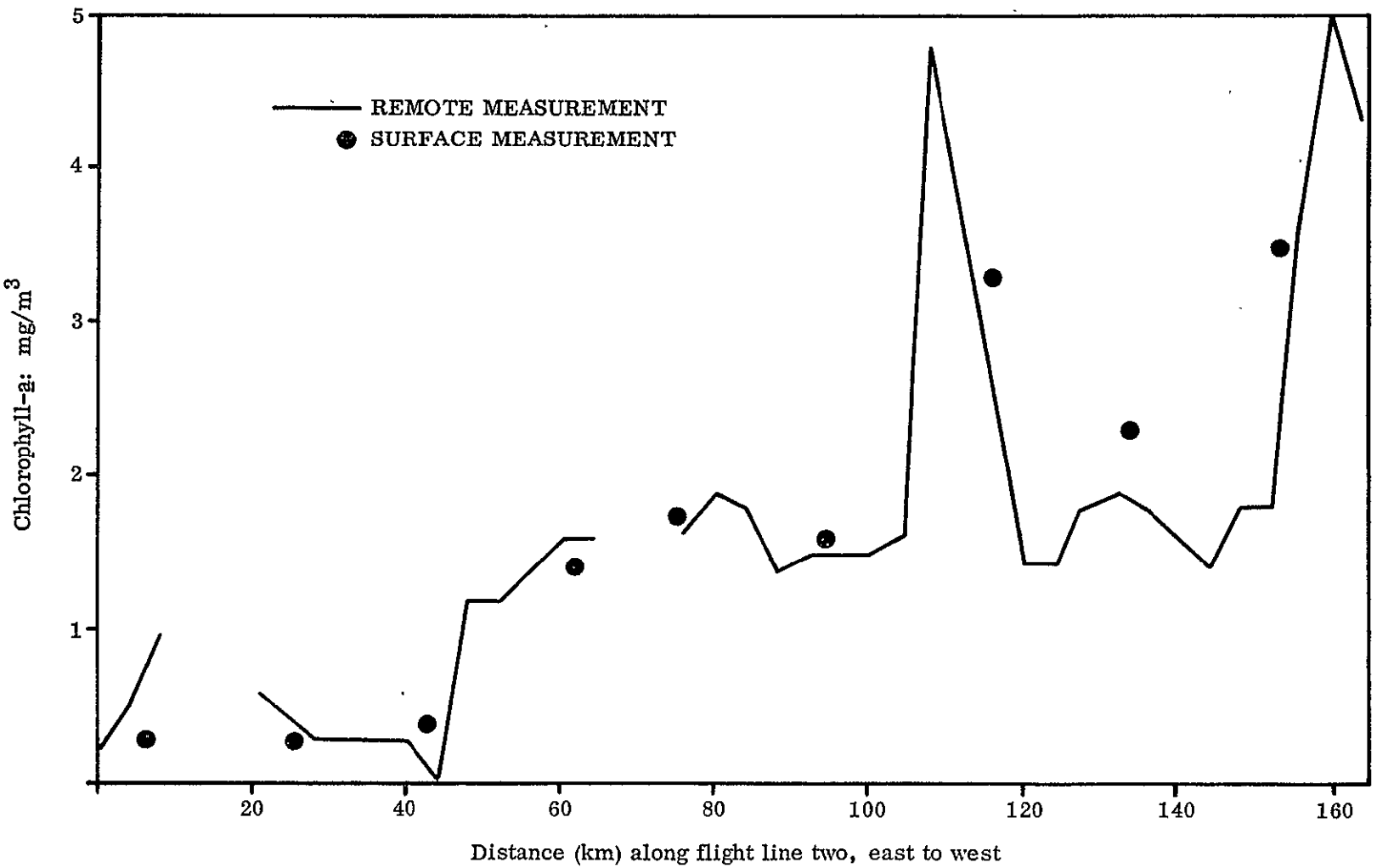

Figure 18. Comparison of Chlorophyll-a Remote and Surface Measurement Profiles Along Flight Line Two

The results are in agreement with the surface measurements as can be seen from Figures 19 and 20 which are contour maps of the Secchi extinction depth made from surface and remote measurements according to this technique. While the calculated rms error was 3.9 meters for 20 points, of which eight were used for calibration, the trends were well represented. The chief discrepancy between the two is in the area where surface readings on the order of 30 meters were made and where the remote measurement indicates greater turbidity.

There are two likely explanations for this variation. Because of the criteria used in selecting calibration points for the remote measurements, which included a maximum time difference between surface and remote measurements of three hours, no calibration points had Secchi depths of more than 17 meters. This would introduce an uncertainty of unknown magnitude into measurements outside the calibrated range. Also, reports from the surface observers indicated that water conditions were changing over the test area. It is thus possible that the sea conditions changed at this sample station during the four hour interval separating surface and remote measurements.

6.3.4 SALINITY

Because salinity is an important factor in the sea truth white marlin predictor to be described later, it would have been desirable to use remote measurements of salinity in this experiment. The feasibility of applying L-band radiometer data to measure salinity remotely has been demonstrated by Thomann (13). Unfortunately, the microwave radiometer necessary for this measurement was not available for use on the aircraft for this experiment; the other potential source for remote salinity measurements was the L-band radiometer on Skylab. However, the footprint of the instrument was almost as large in area as the entire test site, resulting in insufficient resolution.

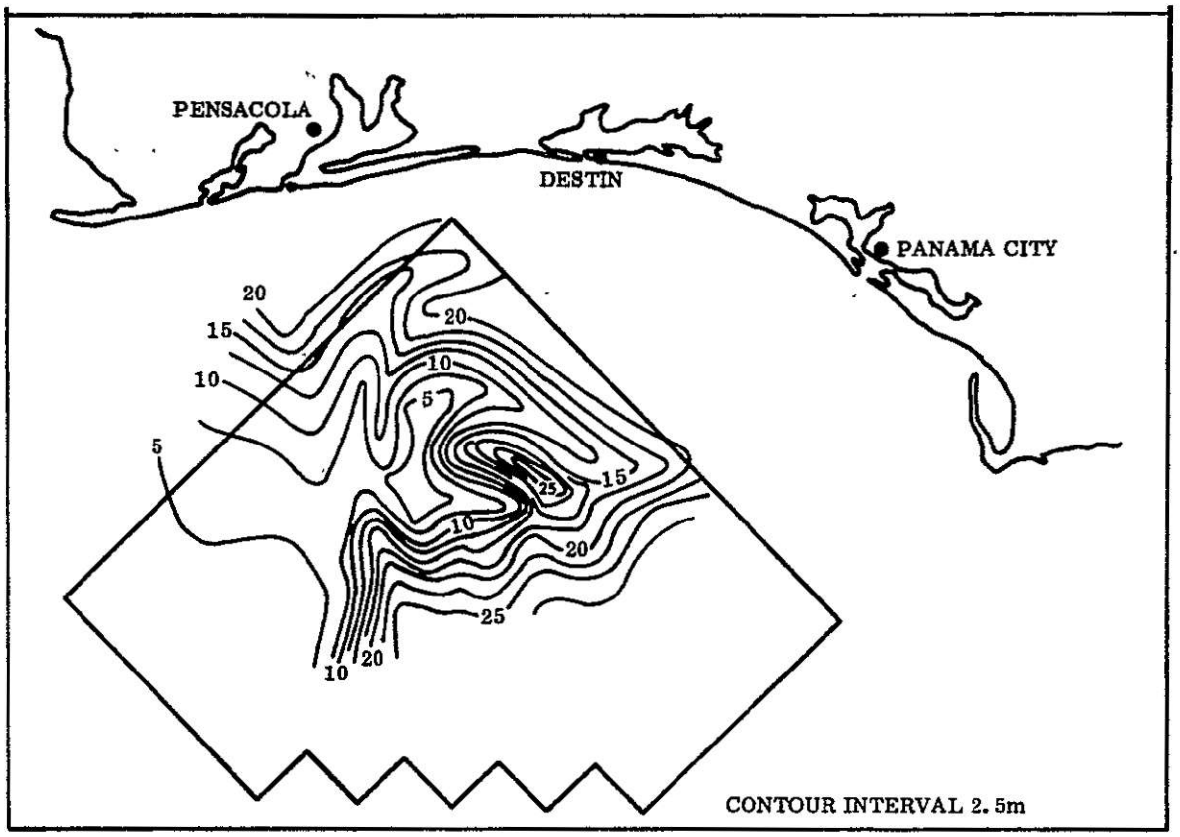

Figure 19.. Surface Measurement of Turbidity (Secchi Extinction)

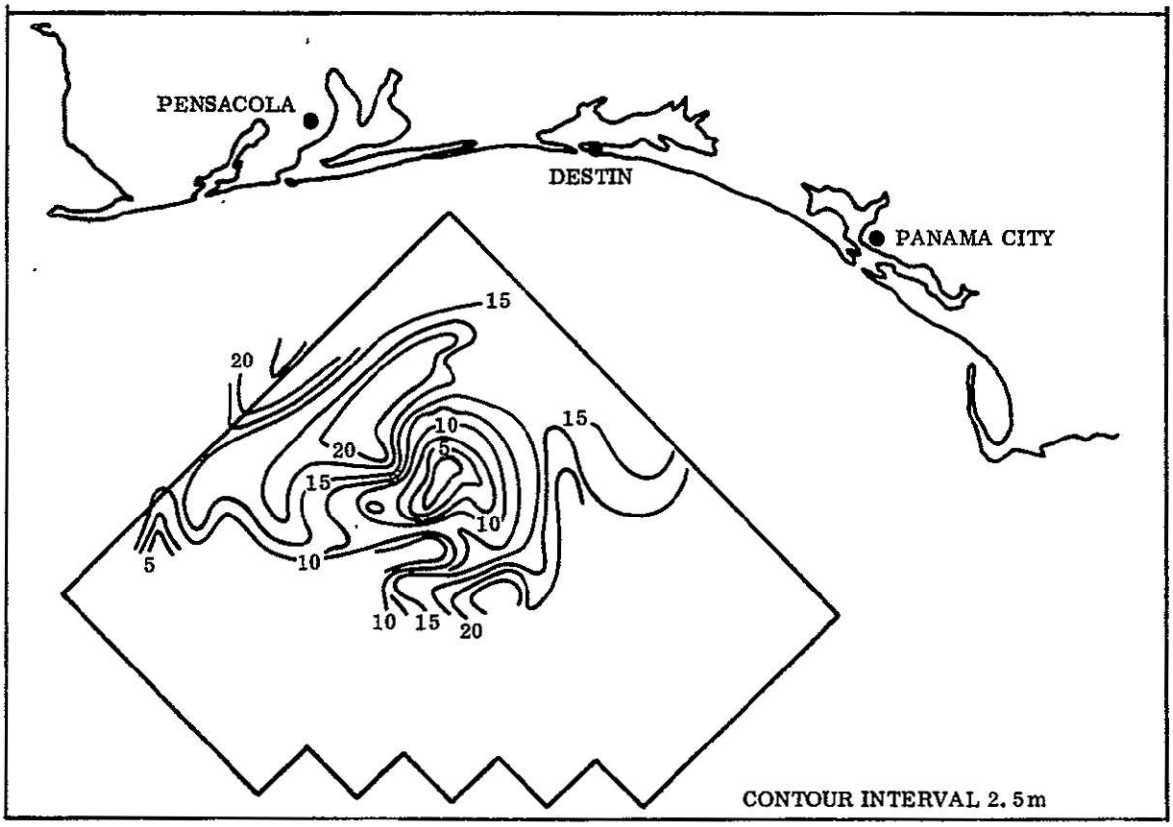

Figure 20. Remote Measurement of Turbidity

6.4 RESOURCE AND REMOTELY SENSED DATA RELATIONSHIPS

6.4.1 APPROACH

Fishermen in search of gamefish consider, as a rule, the color of the sea as the primary indicator of good fishing grounds. The generally accepted theory is that the gamefish are found principally in areas where the water is blue as opposed to green. The approach taken in attempting to define a relationship between the billfish resource and marine phenomena directly sensible by the satellite and aircraft sensors utilized visual interpretation, color enhancement of multiband photography, multiband imagery, and direct correlation between resource distribution information and information from the S191 and S192 systems.

6.4.2 WATER DISCONTINUITIES

The photography from the NC-130B and the light aircraft were visually examined for surface discontinuities which would indicate the boundary between different water masses. The discontinuities searched for were either sharp changes in water color, of which none were found, or surface rips. Many rips were identified, some in both sets of aerial photography. Unfortunately, the portion of the test site visible in the photography was small, therefore much of the study area could not be included in this analysis of the aerial photography.

Figure 21 shows the relationship between rips and white marlin hooked. The fishing squares containing rips are indicated by horizontal lines. Squares where fish were hooked are shade The limited data set does not permit any definitive conclusions to be drawn concerning fish/rip relationships, but one must observe that there were no fish caught in squares containing rips.

No rips were found in the Skylab S190A or S190B photography which has been examined in detail. This is to be expected since these surface features generally have widths less than the resolution of both the S190A and S190B sensors.

6.4.3 S190A PHOTOGRAPHIC SYSTEM

The S190A multispectral photographic system consisted of six high-precision cameras with matched optical systems. Each had an F/2.8 lens with aperture variable to F/16 in 1/2-stop increments and a focal length of 15.2 centimeters (6 inches). At a nominal spacecraft altitude of 435 kilometers (235 nautical miles), the 21.2-degree square field of view provided ground coverage 163 kilometers (88 nautical miles) square. The film width was 70 millimeters, which provided a usable image 5.7 centimeters (2 1/4 inches) square. The camera system compensated for the forward motion of the spacecraft along the flight path. Each of the six cameras was identified by a station number and equipped with combinations of filters and films for the various wavelength bands (Table 12).

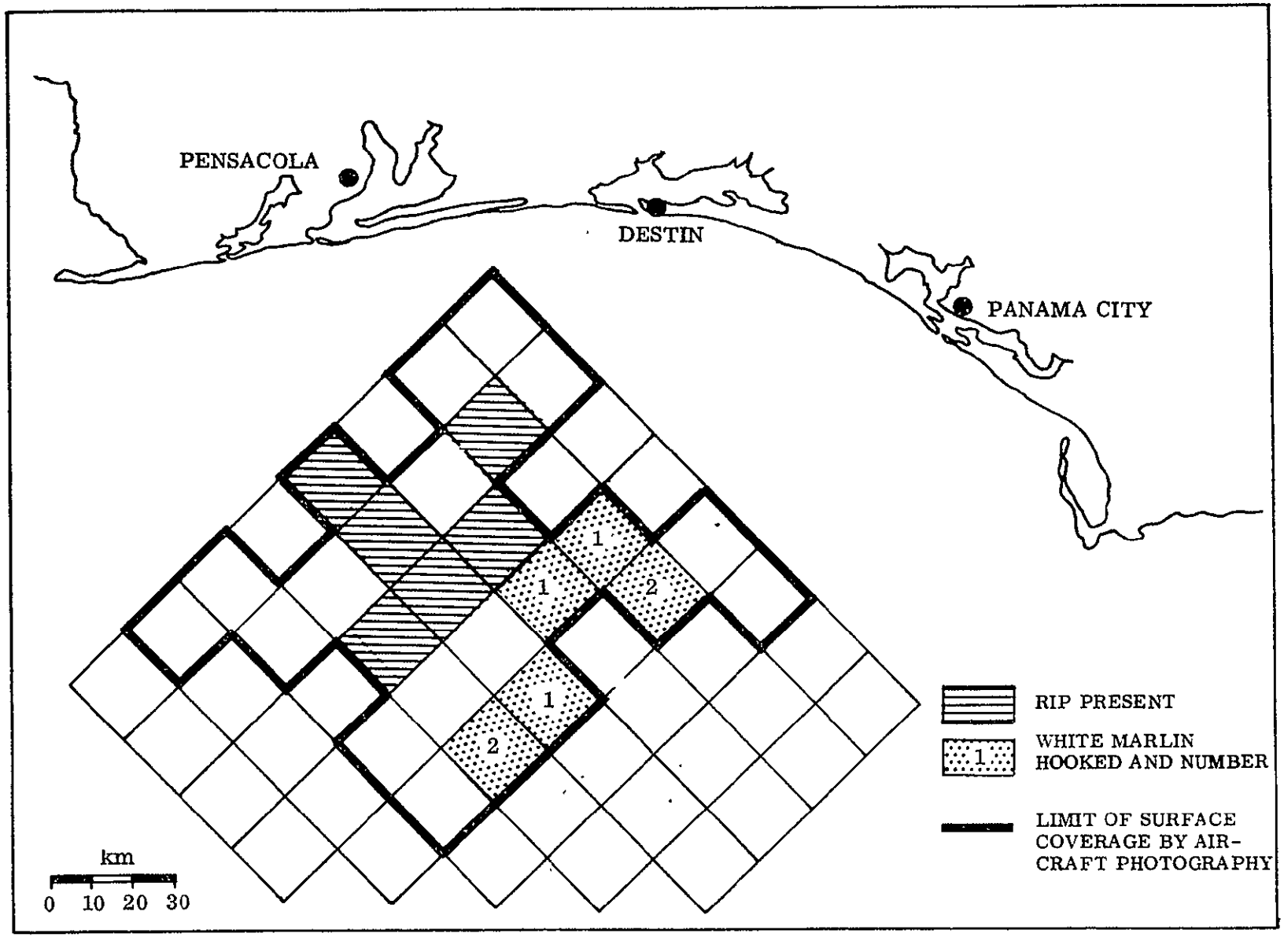

Figure 21. Comparison of White Marlin Distribution with Surface Rip Locations

Table 12. Multispectral Camera Station Characteristics and Film Rolls Used

Sta	Filter	Filter Bandpass, micrometer	Film Type*	Estimated Ground Resolution // meters (feet)	Mission SL-3 Roll No.
1	CC	0.7 - 0.8	EK 2424 (B&W infrared)	73 - 79 (240 - 260)	19
2	DD	0.8 - 0.9	EK 2424 (B&W infrared)	73 - 79 (240 - 260)	20
3	EE	0.5 - 0.88	EK 2443 (color infrared)	73 - 79 (240 - 260)	21
4	FF	0.4 - 0.7	SO-356 (hi-resolution color)	40 - 46 (130 - 150)	22
5	BB	0.6 - 0.7	SO-022 (PANATOMIC-X B&W)	30 - 38 (100 - 125)	23
6	AA	0.5 - 0.6	SO-022 (PANATOMIC-X B&W)	40 - 46 (130 - 150)	24

* Eastman Kodak Company // At low contrast

Positive black and white transparencies of the experimental area for stations 1, 2, 5, and 6 and positive color transparencies for stations 3 and 4, scaled at 1:2,850,000 were received as S190A data products from NASA's Johnson Space Center.

Of the S190A film products acquired and received for analysis, black and white (B&W) 70mm negative transparencies of successive frames 242 and 243 (11:41:04.3 CDT) of all six stations were made and used in density slicing/color enhancement analyses. Neither frame selected would accommodate the entire test area. Figure 22 shows the two frames from station 6 spliced together with the test site overlaid. The S190A photograph revealed a number of anomalous dark patches (27) within the sun-glint areas, the largest of which appeared in grid square numbers 31 and 48. This particular patch was oval shaped; it encompassed a total area of about 570 square kilometers and was associated with calm sea state measurements ranging from 30 to 40 cm.

Initially, two bands, 0.5 - 0.6 μm and 0.6 - 0.7 μm were density sliced to derive sea surface information. Comparing the distribution of hooked white marlin per square with the image sliced into five density levels revealed that fish were hooked in squares having different density levels. The fishery resource data, as summed and positioned to the center of the squares, therefore could not be correlated with any particular density slice of the S190A multiband Skylab photography as originally anticipated.

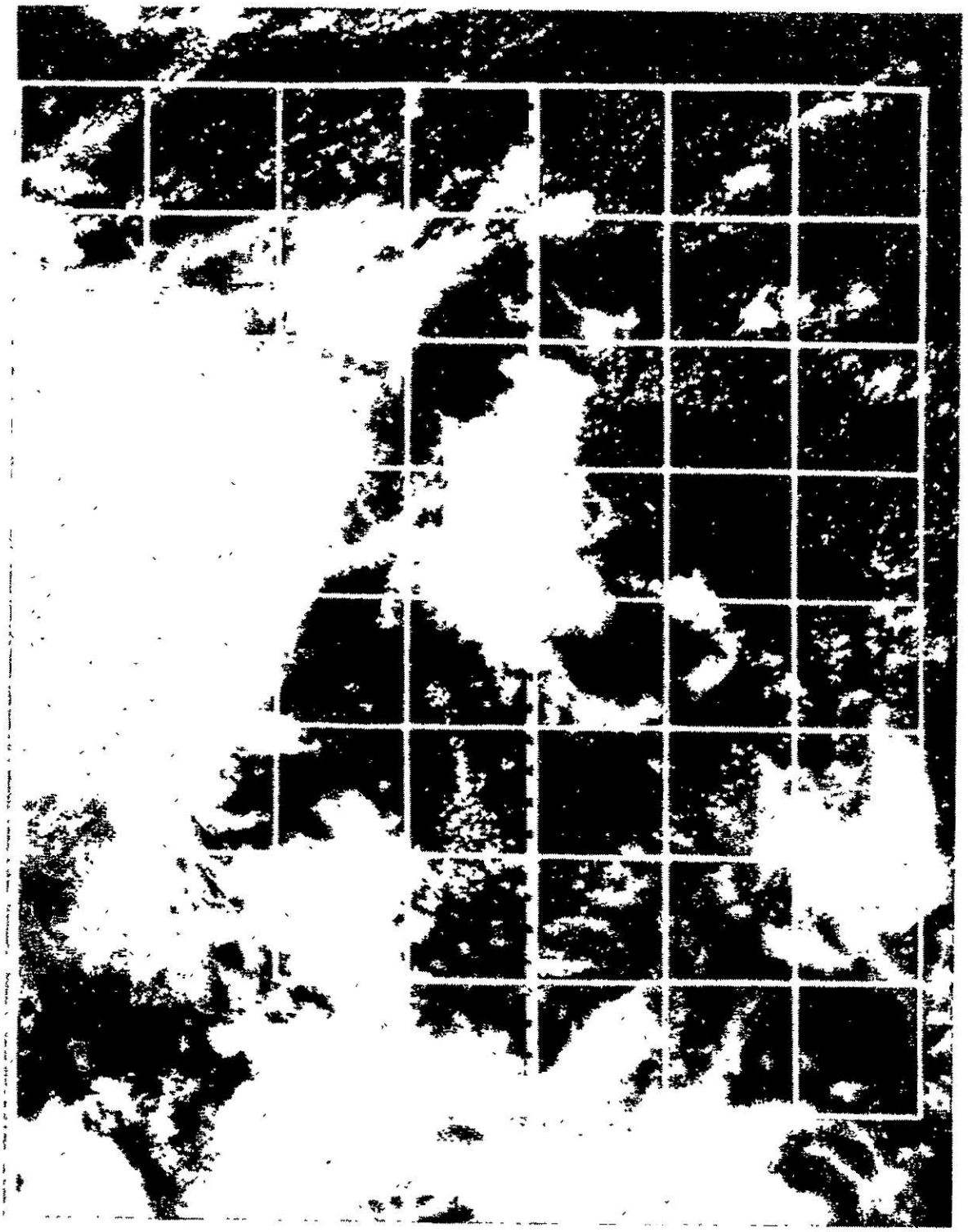

Figure 22. S190A Photography with Test Site and S191 Ground Track Overlay

Further efforts were made to get by this deficiency by utilizing white marlin catch locations accurately to 1/2 mile (twelve in number) determined by electronic navigation equipment aboard a subset of fishing vessels participating in the experiment. A re-examination of the imagery from stations 1 through 6 was made to determine if the distribution of white marlin was located in a particular density region. The image in Figure 22 was density sliced and color coded on a VP-8 image analyzer. The white marlin locations were superimposed and the resulting image photographed and displayed in Figure 23.

Stations 4 and 6 provided better water detail than the other stations, but as can be seen from Figure 23, no density/white marlin relationship could be established. This does not imply that such a relationship does not exist but only that utilizing this set of fishery data and this set of multiband photography, with band widths previously stated, no relationship could be established. More work is needed in this area of analysis before it can be determined if a density/white marlin relationship does exist.

6.4.4 S190B PHOTOGRAPHIC SYSTEM

The S190B earth terrain camera was a single-lens camera assembly having an F/4 lens with a focal length of 45.7 centimeters (18 inches). The camera system was compensated for Skylab's forward motion and had a field of view of 14.24 degrees which produced a square ground coverage of about 109 kilometers (59 nautical miles). Film width was 12.7 centimeters (5 inches), which provides a usable image 11.4 centimeters (4.5 inches) square. On this particular mission, SO-242 (high resolution color) film was used. The filter bandpass was 0.4 - 0.7 μm and the estimated ground resolution at low contrast was 21 meters (70 feet).

Positive color transparencies of the test area approximately 22.86 x 22.86 cm (9 x 9 inches) scaled approximately 1:500,000 were received as S190B data products from NASA's Johnson Space Center.

Negative black and white transparencies from frames 220 and 221 which were spliced together and reduced to approximately 22.86 x 11.43 cm (9 x 4-1/2 inches).

A transparent overlay, containing the test area and that set of white marlin catch locations which could be located to within one-half mile, was prepared and utilized in the density slicing color enhancement analysis as shown in Figure 24.

The clouds (highest reflected radiance) are colored black and sun-glint areas orange. Sun-glint covers a large area in the lower right hand side of frame 220. Water areas were density sliced into three regions and assigned the colors of green, purple and blue going from highest reflected radiance to lowest reflected radiance. Again no relationship between the density of reflected light in the 0.4 to 0.7 μm range and white marlin distribution could be established from a visual evaluation. The sample size of 8 white marlin locations that could be located to .804 km (1/2 mile) accuracy and fairly clear of cloud cover was somewhat small, therefore no attempt was made to compute statistical correlation between fish location and radiance density values.

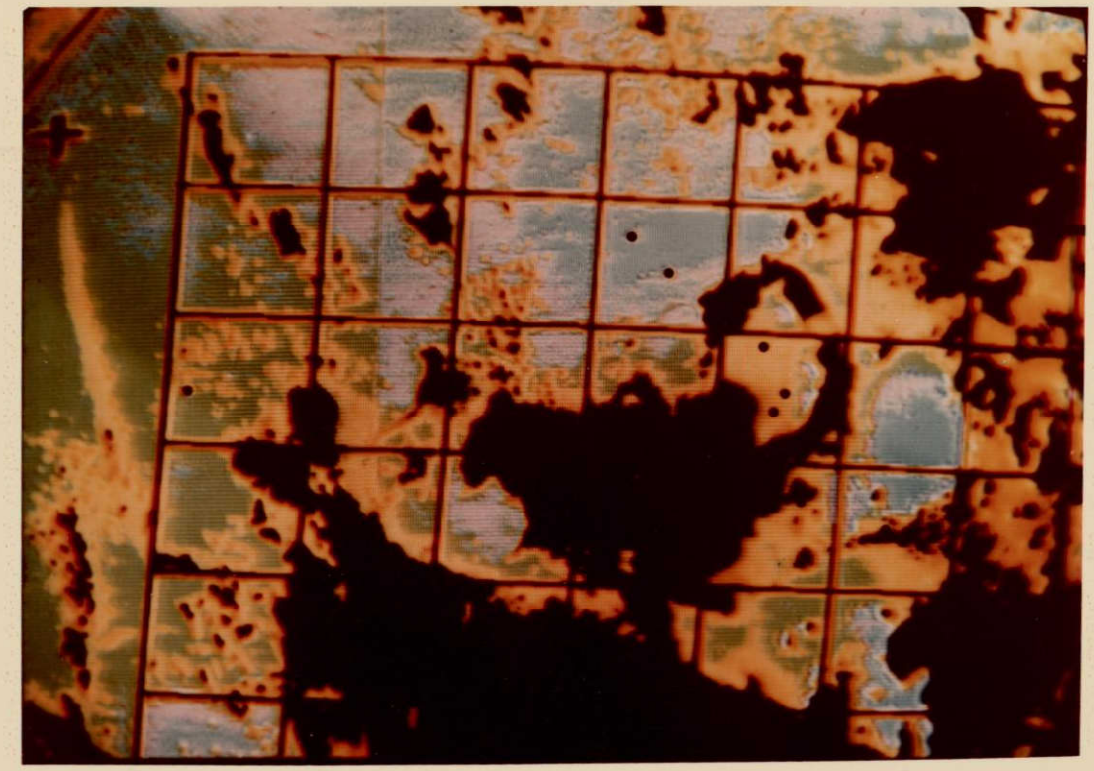

Figure 23. S190A Photography Density Sliced and Color Enhanced with Test Site and White Marlin Locations Superimposed

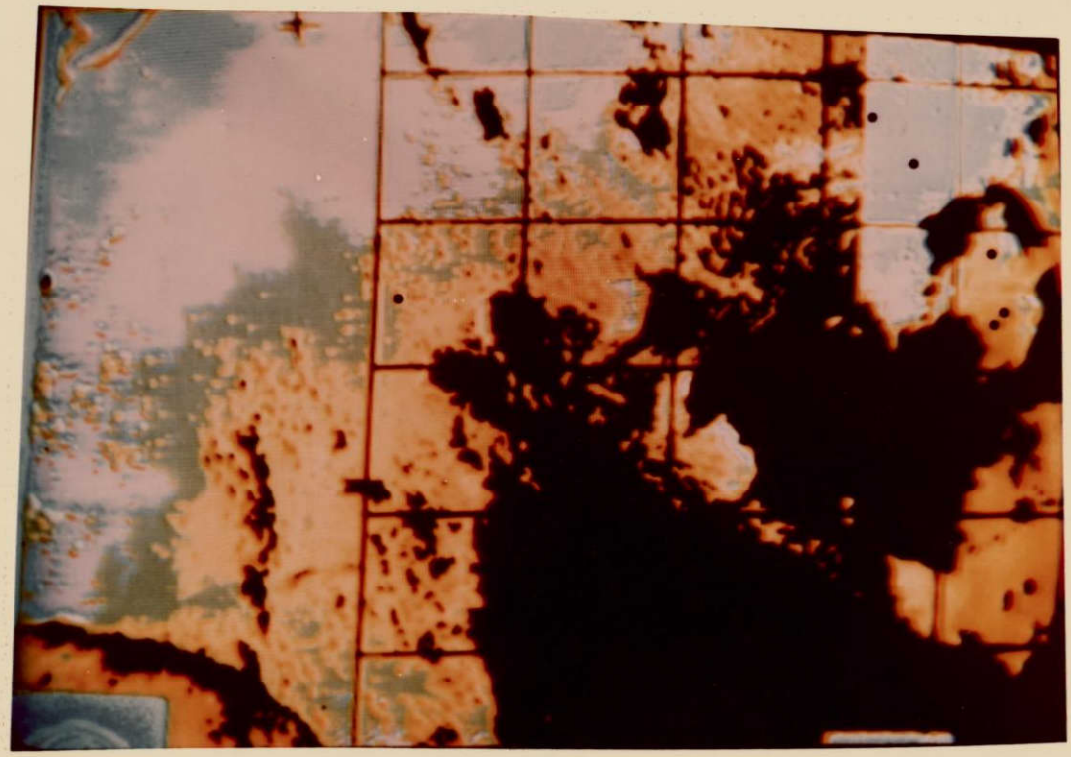

Figure 24. S190B Photography Density Sliced and Color Enhanced with Test Site and White Marlin Locations Superimposed

One promising aspect of the S190B imagery not a part of this experiment was the fact that several of the sportfishing boats could be seen with the naked eye. The fishing boat shown in Figure 25 is 12.5 meters (38 feet) long and was identified by time/position information taken from fishing logs. While the estimated ground resolution of the S190B at low contrast was approximately 21 meters (70 feet), this high contrast target of 12.5 meters (38 feet) shows up quite vividly. From the logs, it could further be established that boats less than 8.9 m (27 feet) could not be seen.

6.4.5 S191 SYSTEM

The S191 sensor is made up of three major elements - a Cassegrainian telescope and plane-mirror optical system that provided an image of the scene to the other two elements, a filter-wheel spectrometer that scanned the radiation from the scene and a boresighted viewfinder and tracking system with the same line of sight as the spectrometer. The infrared sensor's instantaneous field of view was approximately .435 kilometers (.234 nautical miles) in diameter. Incoming radiation was split into short and long-wavelength bands; 0.4 to 2.5 micrometers and 6.6 to 16 micrometers.

Examination of the S191 data acquired over the test area during the Skylab/Gamefish Experiment has revealed that cloud cover obscured major portions of the sensor's coverage along the flight track. This is shown in the S190A station 6 (0.5-0.6μm) imagery with the test site and S191 ground track superimposed. (Figure 22). An isometric presentation of the data from the short wave band (0.4 to 1.1 μm) of the S191 sensor is shown in Figure 26. This presentation of the data represents the information from channel A3, the high gain silicon detector. When the channel saturates, a value of zero is indicated, so when the spectrometer was viewing the very bright clouds and the signal was saturated, the spectrum indicates a zero radiance. Spectra 13 through 35 were taken very near or over the test area. Surface sampling stations were located in areas sampled by the S191 as spectra 13, 15, 18, 20, 22, 25, and 27. Spectra 13 through 15 were cloud free, while spectrum 18 indicates saturation in one portion of the spectrum, due most likely to a small cloud which entered the sensor field of view only briefly. Spectra 19 through 21 appear contaminated, but not saturated. Spectra 22 through 27 are saturated. The rest of the spectra are all contaminated. This limited set of sensor data has prevented further analysis such as development of predictive algorithms for chlorophyll-a and turbidity based on selected S191 spectra.

In addition, initial plans to compute radiance values every 50 nanometers from 0.4 to 0.7 μm range for each 8.05 km (5 mile) subsquare crossed by the S191 flight track resulted in data for only one subsquare. This prohibited any type of statistical analysis between the white marlin distribution and data from this sensor.

6.4.6 S192 MULTISPECTRAL SCANNER

The multispectral scanner was an optical electromechanical scanner which collected incoming radiant energy using a rotating mirror in the image plane to conically scan the scene viewed. The energy scanned in the image plane passed through a reflective Schmidt corrector mirror and through a field stop that was the entrance slit of a prism spectrometer. The short wavelengths (0.41 to 2.43 micrometers) were separated from the long thermal wavelength band (10.2 to 12.5 micrometers) by a dichroic mirror. The spectrally dispersed

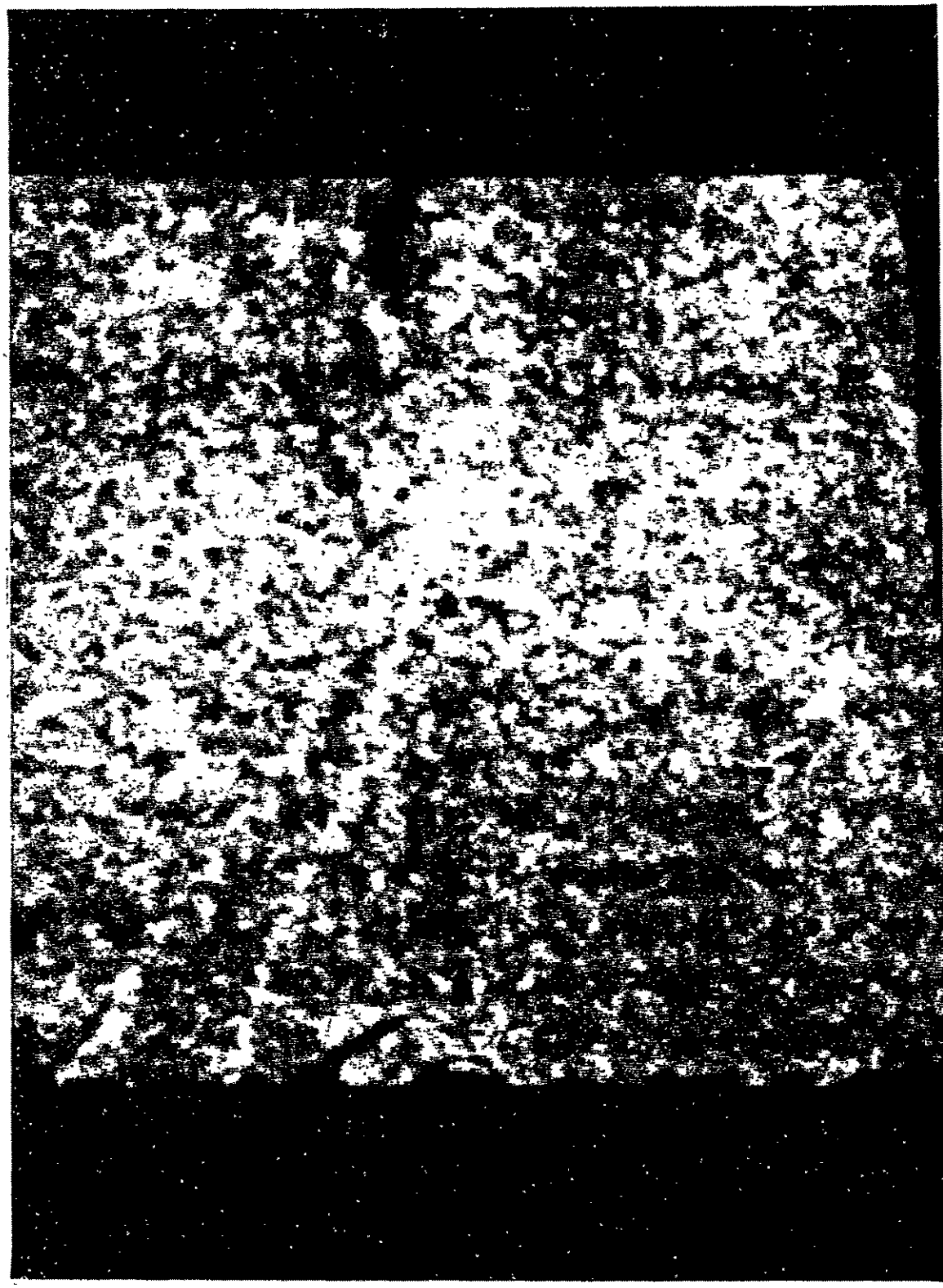

Figure 25. S190 Photograph of Sport Fishing Vessel Magnified 50 Times

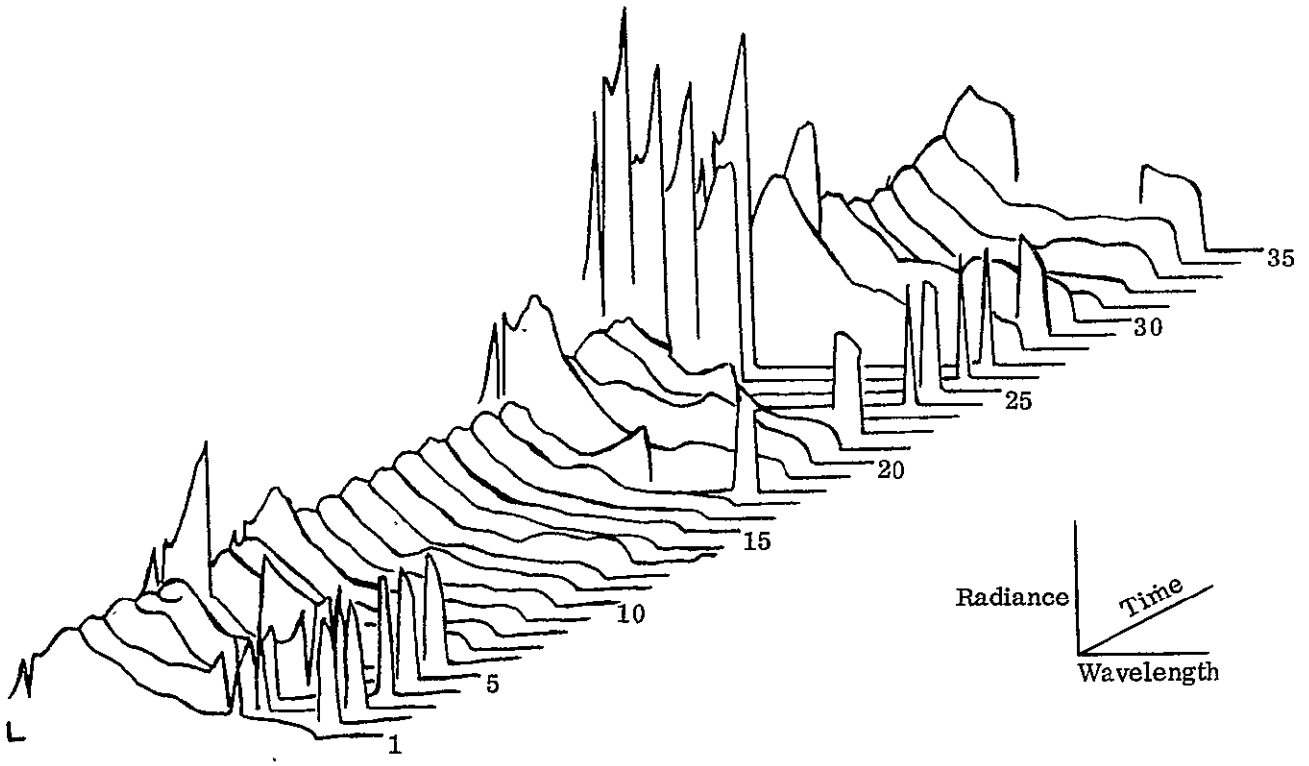

Figure 26. The Isometric Presentation of the Visi n of the S191 Spectra

electromagnetic energy received from the scene irradiated thirteen detectors simultaneously. Detectors and associated wavelengths are listed below:

Band No.	Channel No.	Wavelength, Micrometers
1	22	0.41 - 0.45
2	18	0.44 - 0.52
3	1	0.49 - 0.56
4	3	0.53 - 0.61
5	5	0.59 - 0.67
6	7	0.64 - 0.76
7	9	0.75 - 0.90
8	19	0.90 - 1.08
9	20	1.00 - 1.24
10	17	1.10 - 1.35
11	11	1.48 - 1.85
12	13	2.00 - 2.43
13	21	10.20 - 12.50

Each detector produced an electronic signal that corresponded to the average value of the radiance received in its spectral band from the spot on the surface in the instrument's 0.182 milliradian field of view. The field of view of each detector provided an instantaneous square

ground coverage of 79 meters (260 feet) swept in a conical scan. The ground swath width of the sensor was 74 kilometers (40 nautical miles). The scenes recorded in bands 1 through 11 and 13 are shown in Figures 27 and 28.

Black and white 12.7 centimeter (5-inch) film images of corrected/filtered data from bands 1 through 13 and digital data on tapes from bands 1 through 9 and 13 have been received from NASA-JSC. Evaluation of the S192 imagery resulted in the identification of a ringing of cloud edges across the cloud free areas of the imagery in bands 2, 3, 4, 5, 7, and 8. Discussions with NASA have confirmed that the high frequency filtering of the data created this distortion. Distortion in band 3 can be seen on both sides of the shoreline as waves and out further in the frame as cloud edge duplication. Band 2 is very noisy with frequent scan line dropout. Band 13 is also very noisy and band 1 has data saturation problems.

A request to reprocess bands 1 through 9, and 13 without high frequency filtering in bands 1 through 5, 7 and 8 was submitted to the NASA in April 1975 and the unfiltered data were used in all analysis performed subsequent to receipt of data in June 1975.

Spectral bands 2, 3, and 13 were digitally density sliced. The digital lower and upper count values for channels 2, 3, and 13 on a 0 to 255 count range are listed below.

Channel	Lower Value	Upper Value
2	60	123
3	15	78
13	115	178

These ranges were adjusted to a 0-63 count range and printer plots of the density regions defined below were made and used in conjunction with white marlin distribution data to perform visual correlation analysis.

Density Region	Band 2 and 3 Count Range	Band 13 Count Range
1	0-26 and 63	0-20
2	27-30	21-27
3	31-34	28-35
4	35-38	36-43
5	39-42	44-51
6	43-46	52-63
7	47-50	
8	50-62	

A high level of visual correlation was not observed with any one of the three bands evaluated.

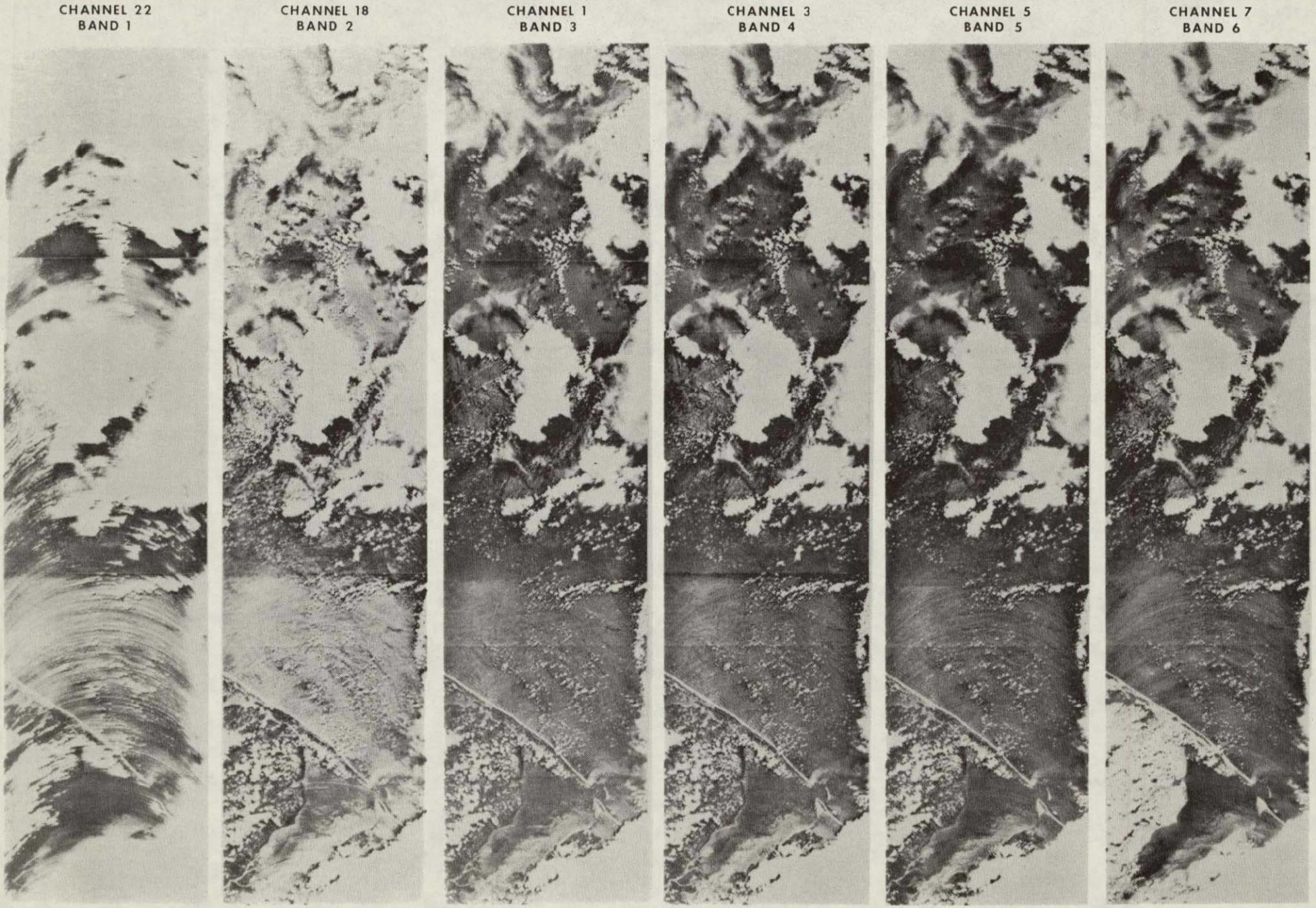

Figure 27. Imagery Taken from Bands 1 through 6 of the S192 System

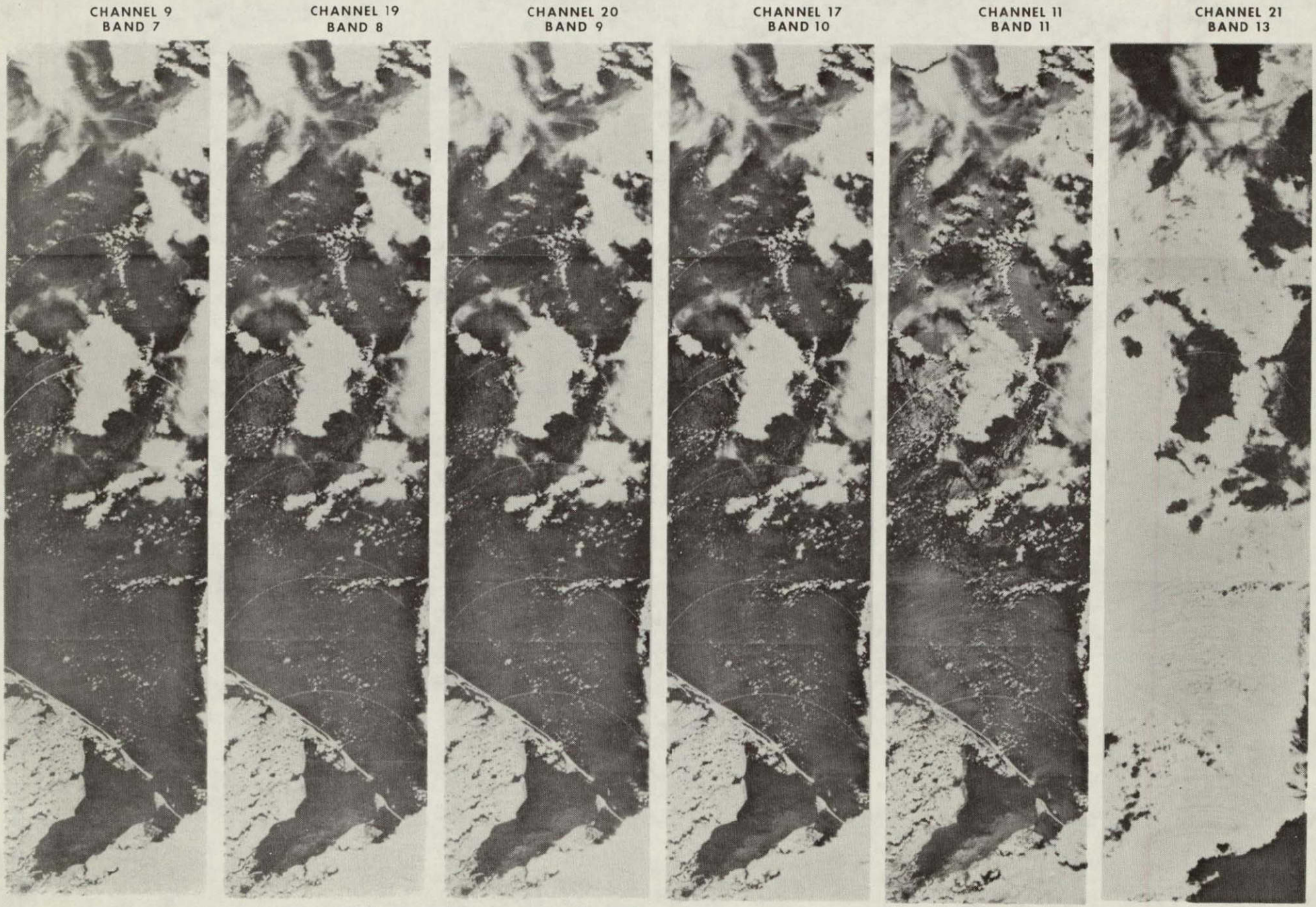

Figure 28. Imagery Taken from Bands 7 through 11 and 13 of the S192 System

SECTION 7

PREDICTION MODELS

7.1 MODEL DEVELOPMENT

Multiple regression analysis was the first technique used to develop models to predict white marlin distribution ($\overline{D}$) in the Skylab test area. Initial runs utilized the eleven parameters listed in Table 13 along with all possible interactions (formed by computing the products of each parameter pair) as the independent parameters. The first models D_1, D_2, D_3 listed in Table 13 were constructed utilizing data collected on 4 August, on 5 August, and the combination of 4 and 5 August. These models were developed based on five parameters: surface water temperature (T), Secchi extinction depth (C), salinity (S) and the two interaction parameters, the product of Secchi extinction depth and chlorophyll-a, (CA), and the product of salinity and surface water temperature (ST). Comparison of constant terms and coefficients (by magnitude and sign) in models D_1, D_2, and D_3 reveal extreme differences from day to day. Therefore, it appeared that important information was not considered, a combination of linear terms was not sufficient to model the day to day changes, or a white marlin distribution model could not be developed.

Additional work was initiated to try to correct this deficiency in the models. Water density was computed and substituted for the product of water temperature and salinity. The latter two had been used in the earlier regression runs. A measure of water density (σ_t) was computed utilizing the following equations (21).

$$C1 = \frac{S-0.030}{1.805} \qquad (d)$$

$$\alpha_o = -0.069 + 1.4708\ C1 - (1.57 \times 10^{-3})\ C1^2 + (3.98 \times 10^{-5})\ C1^3 \qquad (e)$$

$$\Sigma_t = -\frac{(t-3.98)^2}{503.57} \cdot \frac{t+283}{t+67.26} \qquad (f)$$

$$A_t = t\ \left[4.7867 - 0.098185t + (1.0843 \times 10^{-3})\ t^2\right] \times 10^{-3} \qquad (g)$$

$$B_t = t\ (18.03 - 0.8164t + 0.01667t^2) \times 10^{-6} \qquad (h)$$

$$\sigma_t = \Sigma_t + (\sigma_o + 0.1324)\ \left[1 - A_t + B_t\ (\sigma_o - 0.1324)\right] \qquad (i)$$

where: S = salinity in $^o/oo$
t = temperature in °C
σ_t = density parameter

NOTE: Water density (g/cm^3) at observed salinity temperature and 0 meters depth (atmospheric pressure) $= \sigma_t \times 10^{-3} + 1.$

Table 13. Empirical Regression Models Which Predict White Marlin Distribution ($\overline{D}$) in the Skylab Test Area

T = Water temperature (°C)
C = Secchi disc transparency (m)
S = Salinity (ppt)
ST, CA = Interaction formed as the product of the respective parameters

B = σ_t (measure of water density where $\sigma_t \times 10^{-3} + 1$ = water density (g/cm^3))
A = Chlorophyll-a (mg/m^3)
Ri = Radiance from band i (0 to 255 counts)

Model	Inclusive Dates (1973)	n	Regression Model	Standard Error of $\overline{D}$	Model Correlation Coefficient	Significance Level (%)
D_1	4 August	24	$\overline{D} = -419.5394 + 14.3929T + 12.9764S + .0567C - .4461ST + .0074CA$	0.3435	0.797	99.5
D_2	5 August	22	$\overline{D} = 164.1002 - 5.3527T - 6.3246S + .0173C + .2071ST - .0021CA$	0.4996	0.499	50
D_3	4 and 5 August	46	$\overline{D} = - 25.4052 + .9301T + .3258S + .0139C - .0133ST + .0008CA$	0.4751	0.436	75
D_4	4 August	24	$\overline{D} = - 13.3676 + .6583T + .0718C + .3651B + .0043CA$	0.3589	0.762	99.5
D_5	5 August	22	$\overline{D} = - 22.4714 + .8179T + .0143C - .1035B - .0014CA$	0.4879	0.489	60
D_6	4 and 5 August	46	$\overline{D} = - 12.8553 + .4959T + .0142C - .0950B + .0007CA$	0.4693	0.436	90
D_7	5 August	11	$\overline{D} = - 34.4927 + .0264T - .3332\ R_2 + .0722\ R_3 + .1776R_6 + 1.5677R_7$	0.3339	0.892	90

The resulting density measure σ_t was used in constructing models D_4, D_5 and D_6 which also contain surface water temperature, Secchi extinction depth, and the product of Secchi extinction depth and chlorophyll-a. Comparison of the constant term and coefficients reveals a significant improvement in the stability of the coefficient of each parameter from model to model. It should also be noted that the significance level was improved on models D_5 and D_6.

A second technique was also used to model the distribution of white marlin as a function of several environmental parameters. In this case, a discriminant function analysis software package was converted from an IBM 370-65 system to a Univac 1108 system and used to select a subset of the 13 environmental parameters to be used to model white marlin distribution. The parameters which explain the most variation in the distribution of white marlin as selected by the discriminant function routine were sea surface temperature, salinity, Secchi extinction depth and chlorophyll-a for both August 4 and August 5 data sets. These parameters or combination of these parameters are the ones initially selected using the regression routine in the development of models D_1 and D_2. The discriminant function technique results compared well with the results from the regression technique in both the selection of the most important environmental parameters and the evaluation of data in the models. The discrimination software varies from the regression software in that the data must be grouped into fish and no fish sets for the discriminant package and a predictive model is generated for each group based on the data from each group. The regression software accepts one group of data containing both fish and no fish samples and generates a single predictive model for this set of data. Predictive models generated with the discriminant function technique using the four parameters previously listed for both August 4 and August 5 were compared to Models D_4 and D_5. While the discriminant function technique did corroborate the results derived from the regression technique, it did not increase the prediction capability and therefore no further effort was expended in trying to improve the capability to predict white marlin distribution from sea truth data via this technique.

7.2 MODEL EVALUATION

7.2.1 SEA TRUTH

The D_4 and D_5 models were tested with independent test data by using 4 August test data in D_5 (developed from 5 August data) and 5 August test data in D_4 (developed from August 4 data). In each case the resulting unnormalized predicted distribution values (Y) were separated into low, medium and high probability ranges. This was accomplished by computing the mean ($\overline{Y}$) and standard deviation (S) of each set of predicted values. Since evaluation of the two models produced similar results, only the results from the D_5 model are presented in this report. The probability ranges were fixed as follows:

$$\text{Low probability} = Y < \overline{Y} - 1/2S$$

$$\text{Medium probability} = \overline{Y} - 1/2S \leq Y \leq \overline{Y} + 1/2S$$

$$\text{High probability} = Y > \overline{Y} + 1/2S$$

Each predicted value for each test square was classified as low, medium, or high depending on the probability range in which it fell. The actual distribution value for each test

square was assigned a high probability if it had a distribution value of 1 and a low probability if it had a distribution value of 0.

Nine of 24 fishing squares were classified as medium probability areas. Actual fish catch in those nine squares revealed that there existed a 50 percent chance of being in an area that had fish. Considering the extreme of low and high probability regions for model evaluation as shown in Table 14, the model was 93 percent accurate in predicting fish location in the remaining 15 squares.

Table 14. Evaluation Summary for 4 August Predicted Values Using Model D_5

Actual	Predicted	Number of Test Squares
HIGH LOW	HIGH LOW	5 9 = 93% correct
LOW HIGH	HIGH LOW	1 0 = 7% incorrect

Ten of the 24 squares fished produced fish-catch results which revealed that a fisherman had a 42 percent chance of being in a location having fish if a square was randomly selected from the 24 squares. However, if a fisherman selected one of the six predicted high probability squares his chance of being in area having fish increased to 83 percent.

To further determine the value of the predicted high probability squares, an evaluation of these squares with associated abundance data was made. It was found that in the six squares selected by Model D_5 from 4 August data or 25 percent of the test area, 67 percent of the white marlin were hooked in 31 percent of the fishing time.

Visual representations of the predicted values from model D_5 is shown in Figure 29. The number of predicted test squares within a given range having fish are denoted by the shaded areas of solid lines. The number of predicted test squares within a given range not having fish are denoted by the dash lines. Ideally the shaded areas should cluster near the high value or high probability portion of range and the dash line areas near the low value or low probability portion with a very minimum of intersection. The results shown in Figure 29 tend toward the ideal conditions.

The analysis of 4 August data utilizing model D_5 demonstrates the potential for reducing a fishing area by identifying high probability areas. For the cases in point a factor of three or four would be achieved. Furthermore, by only considering high probability areas, the overall probability of being in an area where fish may be hooked, can be increased approximately by a factor of two in the case discussed.

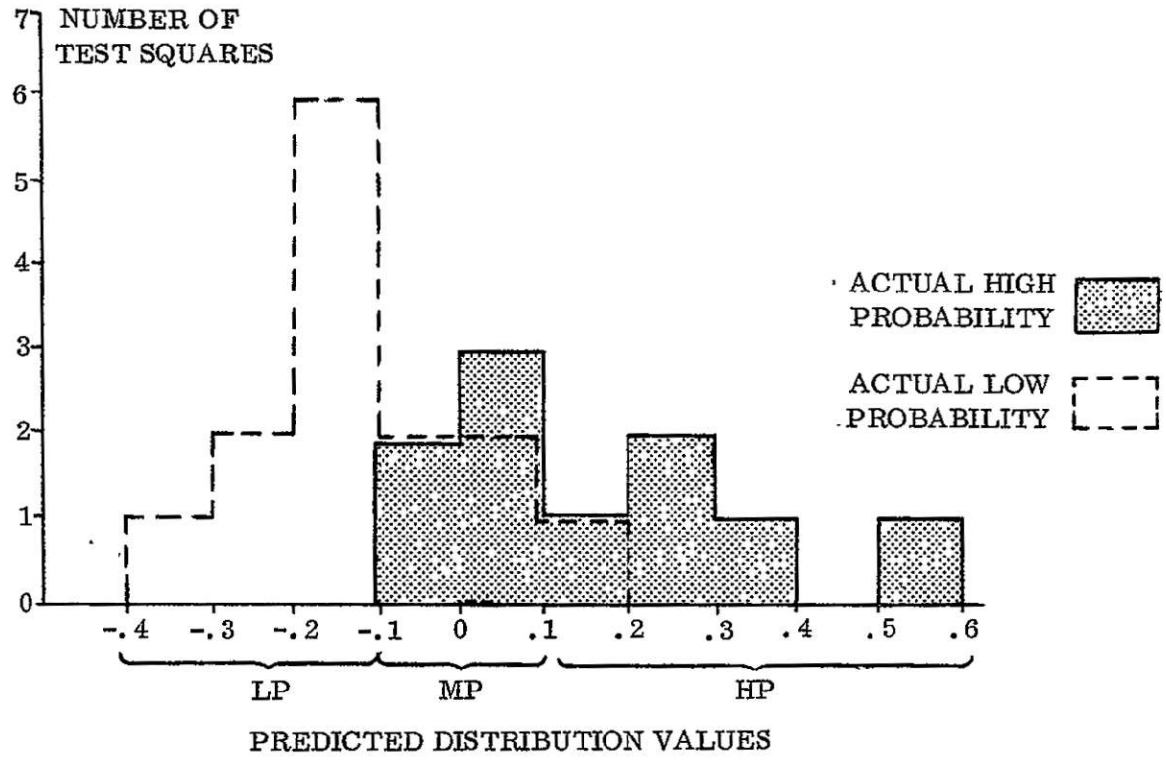

Figure 29. Evaluation of August 4 Predictions, Using August 5 Model D_5

7.2.2 AIRCRAFT REMOTELY SENSED DATA

Data values for remotely sensed sea surface temperature, chlorophyll-a and turbidity were selected from the applicable contour maps. No remotely inferred values for salinity were available so sea truth salinity measurements were used. Water density was computed for each square using remotely sensed temperature and the sea truth salinity. The data values were substituted in Model D_5 and the predicted white marlin distribution values which resulted, were classified as low, medium or high probability areas according to the procedure given in Model Evaluation. Again, not considering the predicted medium probability squares (8 in number) the resulting evaluation is shown in Table 15. The results are probably indicative of errors occurring in one or more of the following processes:

- Selection of data from hand contoured charts of remotely sensed data.
- Use of actual distribution comparison values based over the entire day rather than the plus or minus two hours of the aircraft flight time.
- Extrapolation of values from the narrow footprint coverage of the aircraft sensors.

Table 15. Evaluation Summary for 5 August Predicted Values Using Model D_5 with Aircraft Remotely Sensed Values

Actual	Predicted	Number of Test Squares
LOW HIGH	LOW HIGH	2 1 = 50% correct
LOW HIGH	HIGH LOW	2 1 = 50% incorrect

7.2.3 SATELLITE SKYLAB S192

The final modeling efforts concentrated initially on the distribution of white marlin as a function of the radiance values from bands 1 through 7 and 13 of the S192 sensor acquired on August 5, 1973. Band 1 was not used because of the data saturation and/or poor frequency response documented in the S192 Sensor Performance Evaluation Final Report, May 5, 1975 (29). Band 13 (the thermal band), a very important band as signified by the strong correlation between temperature and white marlin distribution, could not be used due to a noise value of 2.6°K during the SL-3 mission. Sea surface temperature compared quite favorably with aircraft remotely sensed temperature data. Comparison of satellite thermal data to both sea surface temperature and aircraft remotely sensed temperature showed no correlation. The variation in sea truth temperature over the test area was approximately 3°C. The S192 temperature values exceeded the relative measurement of temperature to .1°C needed for white marlin distribution correlation work. This could have been caused by cloud contamination and/or noise levels in the remotely sensed temperature data. Because of the high correlation with temperature, sea truth temperature was used in the place of band 13 along with radiance values from bands 2 through 7 to develop a white marlin distribution model based on as much remotely sensed data as possible. Average radiance values from each channel (2 through 7) for each fishing test square were computed by averaging a 40 by 40 element area with many of the cloud cover elements removed from the average by means of a tolerance testing technique. While all cloud cover elements were not removed, it is felt that only a small number were included. However, there was no way to truly assess the exact number of cloud contaminated elements included in the area. Fishing squares having less than 800 elements after cloud removal were not used. Using these procedures, 11 of the 22 test squares from August 5 were used as the data set to develop model D_7 which is shown in Table 13. The model is based on sea surface temperature, and radiance values from bands 2, 3, 6, and 7. Bands 4 and 5 were eliminated by the regression routine. This elimination was due to a less than 1 percent of the variation in white marlin distribution being explained by either band. The lack of ability of these bands to explain very much variation in the dependent variable may possibly be attributed to the information acquired in these specific spectral windows. System noise requirements of the EIS (End Item Specification) for the S192 sensor was exceeded on both of these bands during SL-3.

The correlation coefficient for Model D_7 was 0.892 which was more than 0.489 for D_2 and 0.489 for D_5. The significance level was 90 percent which exceeded the 50 percent for D_2 and the 60 percent for D_5. The improvements in model D_7 were initially attributed to one of two things. The radiance data from the S192 sensor was doing a better job of explaining the variation in white marlin distribution on August 5 than the additional sea truth parameters or the smaller sample size was affecting the statistics. To answer this question, a model was developed from the same sea truth parameters used in model D_5 except that only the 11 squares in question were used.

The correlation coefficient for this model was .688 which was an improvement over .489 for D_5, but still less than the .892 for D_7. The significance level for this model was 60 percent which was the same as D_5, but less than the 90 percent for D_7. Therefore, the increase in precision of the model can be attributed to the data from the S192 sensor.

Further attempts were made to improve model D_7 by subtracting band 7 from each of the remaining bands used in D_7 (bands 2, 3, 5 and 6). This was done to try to remove the effects of sun glint. Since the band 7 is sensing only surface features, it seems logical that maybe the surface feature of sun glint could be removed from the bands 2, 3, 5 and 6 by the subtraction procedure. The resulting parameters along with band 7 and sea surface temperatures were used to generate a model. The correlation coefficient of this model was .892 and the significance level was 90 percent. Therefore, no apparent improvement was noticed and this procedure was discarded.

The results indicate that the relationship between white marlin distribution and sea truth environmental parameters is more complex than a linear combination of the environmental parameters. However, while only two days of data were available for sea truth modeling efforts, it is evident that the relationship can be modeled with reasonable stability from day to day.

Furthermore, with only one day of remotely sensed data from 4 bands of the S192 and sea surface temperature, a significant improvement was made in modelling the distribution of white marlin for the August 5 data set. While the noise level on band 13 far exceeded levels which would permit its use, aircraft sensors can remotely measure temperature to the necessary levels (.1°C relative in the case of white marlin for this particular time period). Present satellites such as NOAA's ITOS (G-D) (30) can measure temperatures relative to .5°C and near future satellites such as LANDSAT C* will also be able to measure temperatures (relative) to .5°C for a certain range of temperature. Satellites such as these could one day be used for fishery resource assessment and monitoring application programs.

Since there was only one day during which satellite remotely sensed data was acquired, no independent data exist for model verification. The only test which could be made was to input the August 5 remotely sensed data from bands 2, 3, 6, 7 and sea truth temperature into multiple regression model D_7 and compare the predicted white marlin distribution values to the actual white marlin distribution values. The actual distribution values for white marlin

*Personal conversation with Dr. Stan Fredden, NASA, Goddard.

are shown in column Y and the predicted white marlin values in column PY. Test samples having fish in the actual column had a value of 1 assigned and those not having fish had a value of 0 assigned as shown in the table below.

SAMPLE	Y	PY
1	1.0	.82
2	1.0	.90
3	1.0	.99
4	1.0	.97
5	1.0	.76
6	0.0	.04
7	0.0	-.20
8	0.0	.42
9	0.0	.44
10	0.0	.07
11	0.0	-.20

It is clear that the predicted values can be separated into two categories; fish and no fish.

The eleven test samples were also classified via discriminant function technique by computing posterior probability and square of Mahalanobis distance. The results are shown in the following table.

GROUP WITH LARGEST PROBABILITY		SQUARE OF DISTANCE (D) FROM AND POSTERIOR PROBABILITY (P) FOR GROUP -			
GROUP FISH. CASE.		FISH		NO FISH	
		D	P	D	P
1	FISH	2.900	.995,	13.432	.005,
2	FISH	5.223	.999,	18.534	.001,
3	FISH	5.470	1.000,	21.551	.000,
4	FISH	7.175	1.000,	22.619	.000,
5	FISH	1.785	.988,	10.560	.012,

GROUP NO FISH CASE -		FISH		NO FISH	
		D	P	D	P
1	NO FISH	19.552	.001,	4.945	.999,
2	NO FISH	26.090	.000,	3.643	1.000,
3	NO FISH	7.171	.243,	4.903	.757,
4	NO FISH	4.431	.291,	2.654	.709,
5	NO FISH	16.167	.001,	2.519	.999,
6	NO FISH	26.211	.000,	3.772	1.000,

Again, the samples were easily classified using this procedure. Therefore, indeed there is something unique about areas with fish and areas without fish which allows a separation of these areas via certain measured parameters and some specialized classification techniques.

7.3 APPLICATIONS

Considerations relative to the application of the model to wide areas may be categorized as both spatial and temporal. The sea truth parameters as well as remotely measured parameters used in the model were selected because they applied significantly to the white marlin resource in the Gulf of Mexico during the time frame of data acquisition. Elsewhere in the world, for other species and possibly different time frames, other parameters might figure more importantly. The models would require rework using the parameters most applicable to the particular area or possibly using the same set with additional parameters representing the unique, environmental characteristics identified with that area.

The relatively narrow range of values used in model development is another factor presently limiting use elsewhere except where the environment is analogous to that of the Gulf of Mexico during the month of August or during time periods where the ranges of the parameters were not exceeded. For example, the sea truth measurement of sea surface temperature varied from 28.5°C to 31.6°C during the data acquisition operations. For temperature values outside that band, it is unclear if the model performance would be adequate. This is true about each parameter used in the models.

The models are based on data taken during the limited, two day operations and which covered a very small portion of the total range of each parameter. It is questionable how well the models would function with data outside the range of the data with which they were developed. However, since parameter range is obviously associated with seasonal weather (except in the tropics), model inadequacy with respect to data range may be considered a temporal deficiency which could be corrected by the input of additional data collected during other seasons of the year.

The models could be tested elsewhere than in the Gulf of Mexico to resolve the question of spatial deficiency. For example, white marlin are fished quite heavily along the southern Atlantic Coast which could be used as second test area from which to collect data. Future investigations could well include both temporal and spatial testing of the relationship between white marlin and the environment.

Oceanic gamefish distribution prediction models of the type reported herein would clearly serve sportsfishermen and resource managers. Knowledge of highest potential catch areas as a function of time will provide sportsfishermen with the benefits of increased catch and decreased time and fuel expenditures. Figure 30 is an example of a prediction model product which displays fishing areas in terms of catch potential.

These prediction models are presently not adequate in terms of functional operation for resource management applications. Daily operational utilization of these models must wait until remotely sensed data such as the spectral bands utilized in model D_7 can be acquired on a synoptic basis and transmitted on a daily basis to utilization points similar to the present weather satellite systems.

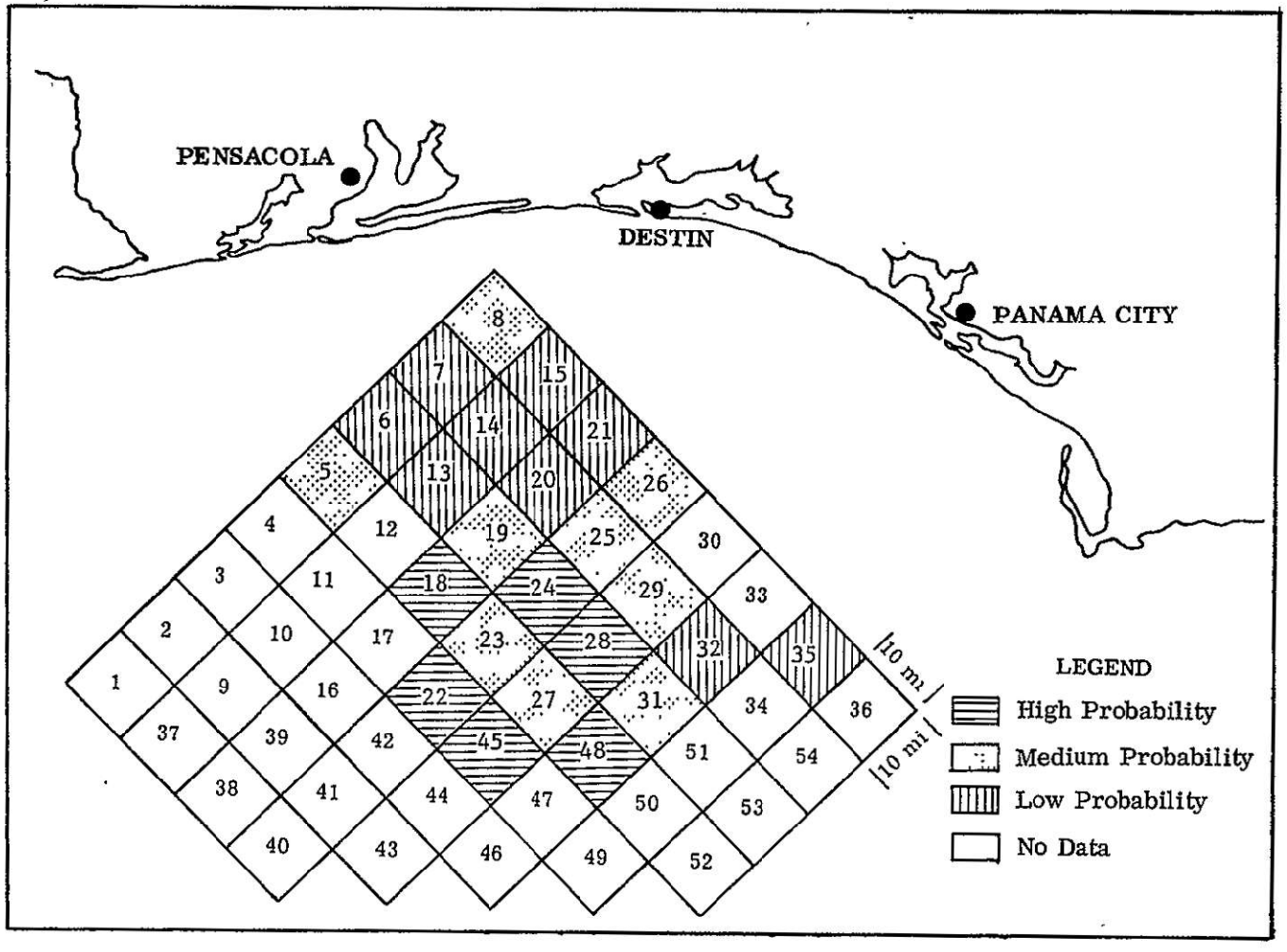

Figure 30. Prediction Results of August 4 Data Using Model D_5

As models are improved and as repetitive data acquisition becomes economically feasible, it is reasonable to presume that these or similar models could provide the abundance and distribution information necessary for development of conservation and harvesting procedures. As operational readiness and confidence in such models are established, resource managers would have additional information on which to base domestic and international conservation decisions.

SECTION 8

CONCLUSIONS

The distribution and abundance of white marlin correlated with the chlorophyll, water temperature and Secchi depth sea truth measurements. Results of correlation analyses for Dolphin were inconclusive.

Prediction models for white marlin were developed using step-wise multiple regression and discriminant function analysis techniques which demonstrated a potential for increasing the probability of gamefishing success. The models also demonstrated a potential for significantly reducing a sportsman's search time by identifying areas that have a high probability of being productive.

Chlorophyll-a, sea surface temperature and turbidity (Secchi extinction depth) values were inferred from aircraft sensor data. Comparisons with sea truth measurements revealed that reasonable accuracy can be expected even in unfavorable atmospheric conditions.

The usefulness of the Skylab S190A and S190B imagery was inhibited by cloud cover and sun glint in the test area on August 5, 1973. The S190A and S190B imagery was density sliced/color enhanced with white marlin location superimposed on the image, but no density/white marlin relationship could be established. The resolution of the S190B imagery was sufficient to see fishing boats 12.5 meters (38 feet) in length, demonstrating a potential for use in fishery remote sensing surveillance systems. The S191 data are insufficient for detailed fishery analysis.

Evaluation of the S192 multispectral data revealed a significant problem associated with high frequency filtering. The S192 data was reprocessed without high frequency filtering in bands 1 through 5, 7 and 8. Data from spectral bands 2, 3, and 13 were digitally density sliced and the white marlin location superimposed on the grey level images; again, no visual relationship could be established using this single channel visual correlation approach. Both multiple regression and discriminant function techniques were used to successfully develop a white marlin distribution prediction model (D_7) based on sea surface temperature and radiance values from S192 spectral bands 2, 3, 6, and 7. This is the first fishery distribution prediction model to use direct satellite measurements, and it shows significant improvement over models for the same time period based solely on sea truth measurement.

From the set of data analyzed in this experiment, surface water temperature was the most important single parameter with respect to correlation with white marlin distribution. Unfortunately the thermal data from the S192 sensor on SL-3 had noise levels which disallowed its use. Relationships between temperature and white marlin distribution indicate that relative temperatures must be accurate to .1°C. This, of course, was based on data taken in August in the Gulf of Mexico where the water surface temperature range is very small (approximately 3°C on August 5, 1973). With larger temperature ranges (different time or location), present satellite (NOAA II) or near future satellite (LANDSAT C) measurements of temperature to .5°C may well suffice for inputs to these types of models.

Based on the results of the satellite remote sensing fisheries investigations to date, it appears desirable to have more spectral resolution for fisheries applications even if it is necessary to sacrifice spatial resolution. It would also be desirable, in future fishery application programs, to acquire daily satellite synoptic observations. The daily acquisition of satellite synoptic observations would greatly enhance the chances for successful acquisition of remotely sensed data concurrent with the acquisition of data from the biological source under investigation.

Correlation analyses have shown that there is a relationship between sea surface parameters and remotely sensed information and gamefish distribution. Models developed using this information enhance our capability to predict high catch probability areas for gamefish.

With the successful identification of fisheries significant oceanographic parameters, the demonstration of the capability of measuring most of these parameters remotely, and the utilization of both oceanographic and satellite remotely sensed data to develop and test white marlin distribution models, the experiment's main objective of establishing the feasibility of utilizing remotely sensed data to assess and monitor the distribution of oceanic gamefish has been accomplished.

REFERENCES

1. Application of Remote Sensing for Fishery Resource Assessment and Monitoring, Skylab Experiment No. 240. Monthly Progress Reports, May 1973 through October 1975. NMFS FEL documents. MTF, Bay St. Louis, MS p(var)

2. Description of Participation of the Earth Resources Laboratory at Mississippi Test Facility, 1973. NASA ERL document. MTF, Bay St. Louis, MS p(var)

3. Project Plan Oceanic Gamefish/Skylab Project Experiment No. 240, 1973. NMFS FEL document. MTF, Bay St. Louis, MS 133p

4. Woods, E. G. and Cook, P.C., 1973, Skylab Oceanic Gamefish Project. Sixteenth Annual International Gamefish Research Conference, 73 p.

5. Naughton, J.J , 1973. Investigations of Billfish Biology at the Hawaiin International Billfish Tournament. Marine Fisheries Review, Vol. 35. No. 8, 7 p.

6. Fox, W.W., 1971. Temporal-Spatial Relationships among Tunas and Billfishes Based on the Japanese Longline Fishery in the Atlantic Ocean 1956-1965. Sea Grant Tech. Bulletin No. 12, 77 p.

7. Skylab Oceanic Gamefish Project. Interim Data Report. 1973. NMFS FEL document. MTF, Bay St. Louis, MS 3301

8. Skylab EREP Investigators' Data Handbook prepared by Lyndon B. Johnson Space Center, Houston, Texas, 1973. 120 p.

9. Daughtrey, K. R., 1973. Techniques and Procedures for Quantitative Surface Water Temperature Surveys using Airborne Sensors. Earth Resources Laboratory, Report 80, Mississippi Test Facility, 30 p.

10. Worthington, H.T., 1973. Remote Measurement of Surface Water Temperatures in Coastal Waters, NASA Earth Resources Laboratory, Report 85, Mississippi Test Facility, 33 pp.

11. Jones, J.B., 1973. Determination of Chlorophyll Content of Water. Lockheed Electronics Corporation, Technical Memorandum DATM-061, Mississippi Test Facility, 7 p.

12. Weldon, J.W., 1973. Remote Measurement of Water Color in Coastal Waters, NASA Earth Resources Laboratory, Report 83, Mississippi Test Facility, 47 p.

13. Thomann, G. C., 1973. Remote Measurement of Salinity in an Estuarine Environment, Remote Sensing of Environment 2, 249 p.

14. Oceanic Gamefish/Skylab Project Field Operating Plan for Operations 4-5 August. NMFS FEL document. MTF, Bay St. Louis, MS 155p

15. Savastano, K. J., Pastula, E. Jr., Woods, G., and Faller, K. H., 1974. Preliminary Results of Fisheries Investigation Associated with Skylab-3, Ninth International Symposium on Remote Sensing of Environment, Environmental Research Institute of Michigan, 30 p.

16. Savastano, K. J. and Leming, T. D., 1975. The Feasibility of Utilizing Remotely Sensed Data to Assess and Monitor Oceanic Gamefish, 40 p.

17. Kemmerer, A. J., Benigno, J. A., Reese, G.B., and Minkler, F.C., 1973. A Summary of Selected Early Results from the ERTS-1 Menhaden Experiment, NASA CR-133152, 37 p.

18. Wise, J.P., and Davis, C.W., 1973. Seasonal Distribution of Tunas and Billfishes in the Atlantic. NOAA Technical Report NMFS SSRF-662, 24 p.

19. Gibbs, R.H., Jr., 1957. Preliminary Analyses of the Distribution of White Marlin, Makarna albida (Poey), in the Gulf of Mexico. Bulletin of Marine Science of the Gulf and Caribbean 7-(4), 10 p.

20. Gulf of Mexico Its Origin, Waters, and Marine Life. Fishery Bulletin 89, Vol. 55, 1954. 601 p.

21. De Sylva, D. P. and Davis, W. P., 1963. White Marlin, Tetrapturus albidus, in the Middle Atlantic Bight, with Observations on the Hydrography of the Fishing Grounds, Copeia, No. 1, 18 p.

22. Boudreau, R.D., 1972a. A Radiation Model for Calculating Atmospheric Corrections to Remotely Sensed Infrared Measurements. NASA Earth Resources Laboratory Report 14, Mississippi Test Facility, 71 p.

23. Boudreau, R.D., 1972b. Correcting Airborne Scanning Infrared Radiometer Measurements for Atmospheric Effects. NASA Earth Resources Laboratory Report 29, Mississippi Test Facility, 34 p.

24. Worthington, H.T., 1974. Personal Communication

25. Clark, G.L., Ewing, G., and Lorenzen, C., 1970. Spectra of Backscattered Light from the Sea Obtained from Aircraft as a Measure of Chlorophyll Concentration. Science, 167, p. 3921

26. Hovis, W.A., Forman, M.L., and Blaine, L.R., 1973. Detection of Ocean Color Changes from High Altitude, Goddard Space Flight Center Internal Technical Memorandum TMX-70559, 25 p.

27. McClain, E.P. and Strong, A.E., 1969. On Anomalous Dark Patches in Satellite-Viewed Sunglint Areas, Monthly Weather Review, Vol. 97, No. 12, pp 875-884.

28. Knudsen, M., 1962. The Determination of Chlorinity by the Knudsen Method, Reprint by G.M. Manufacturing Company, 63 p.

29. Schwalb, A., 1972. Modified Version of the Improved TIROS Operational Satellite (ITOS D-G). NOAA Technical Memorandum NESS 35.

30. MSC-05546, 1975. Earth Resources Experimental Package - Sensor Performance Evaluation - Final Report, Vol. III (S192).

BIBLIOGRAPHY

Ostle, B., 1963. Statistics in Research, Second Edition, The Iowa State University Press, 585 p.

Rivas, L.R., 1973. Preliminary Fishery Results of Skylab Oceanic Game Fish. Sixteenth Annual International Game Fish Research Conference, October 30, 1973. 1 p.

Sea Remote Sensing Program, Oceanic Gamefish/Skylab Project, Experiment No. 240, 4 and 5 August 1973. Surface Measurements, NASA ERL Rept. No. 082. MTF, Bay St. Louis, MS, 49 p.

Sea Remote Sensing Program, Oceanic Gamefish/Skylab Project, Experiment No. 240, 4 and 5 August 1973, Light Aircraft Operations, NASA ERL Rept. No. 111. MTF, Bay St. Louis, MS, 25 p.

Sea Remote Sensing Program, Oceanic Gamefish/Skylab Project, Experiment No. 240, 2 June 1974, Surface Measurements, NASA ERL Rept. No. 069. MTF, Bay St. Louis, MS, 16 p.

Sea Remote Sensing Program, Oceanic Gamefish/Skylab Project, Experiment No. 240, 30 April 1974. NC130B and Skylab-3 operations, 4 and 5 August 1973. NASA ERL Prel. Rept. 113. MTF, Bay St. Louis, MS p(var).

Sperry Rand Univac Large Scale Systems, Stat-Pack, Programmers Reference UP7502-Rev. 1, p(var).

Spiegel, M. R., 1961. Schaum's Outline of Theory and Problems of Statistics, McGraw-Hill, 359 p.

Stevenson, W. H. and Pastula, E. J., Jr., 1973. Investigation Using Data from ERTS-1 to Develop and Implement Utilization of Living Marine Resources, Final Rept. NMFS FEL document. MTF, Bay St. Louis, MS, 185 p.

Yentsch, C. S., 1960. The Influence of Phytoplankton on the Color of Sea Water, Deep-Sea Research, Vol. 7, p. 1.

Faller, K. H., 1974. Remote Sensing of Oceanic Parameters During the Skylab Gamefish Experiment, Report No. 119, 59 p.

APPENDIX A

GAMEFISH BOAT LOGS
OCEANOGRAPHIC DATA ACQUISITION FORMS
GAMEFISH LOADING FORM

OMB No. 41 S73039
Approval Expires 12/31/73

GAMEFISH BOAT LOG

BOAT NAME _____ CAPTAIN _____ DATE _____

REF. NO.	OCEANIC GAMEFISH	TIME				BAIT	WATER COLOR	RIP, OPEN WATER, SCATTERED GRASS, DEBRIS
		RAISED	HOOKED	LOST	BOATED			
1.								
2								
3.								
4.								
5.								
6.								
7.								
8.								
9								
10								

SQUARE NO.	LINES IN	LINES OUT	NO. RODS FISHED	ROD HOURS FISHED - BAIT				
				MULLET	BALLYHOO	STRIP	ARTIFICIAL	OTHER

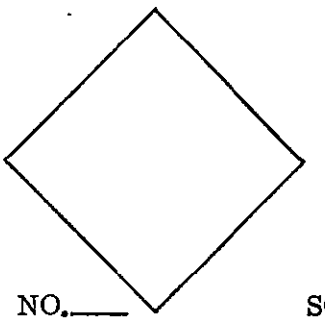
SQ. NO.____

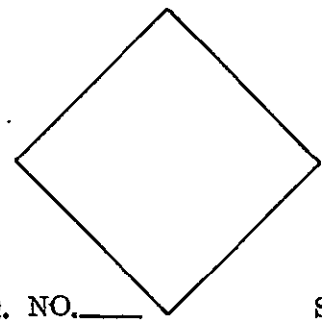
SQ. NO.____

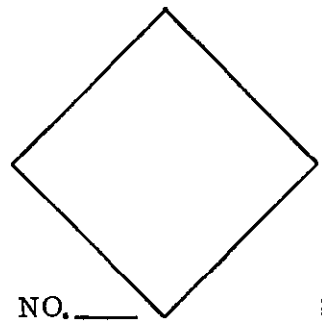
SQ. NO.____

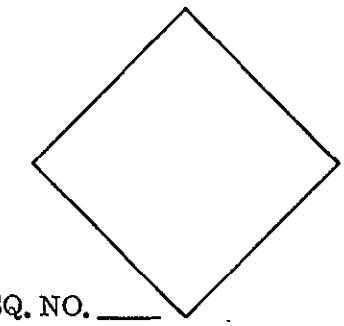
SQ. NO.____

GAMEFISH BOAT LOG

BIOLOGICAL DATA

(TO BE FILLED OUT BY PORT SAMPLER)

BILLFISH SPECIES	TIME HOOKED	GIRTH (cm)	SEX	WEIGHT (LBS.)	LENGTH (cm)	
					LOWER JAW TO FORK	ORBIT TO FORK

BILLFISH SEEN: YES_____ NO _____

IF YES: TIME _____ SPECIES _____ SQUARE NO. _____

_____ _____ _____

GAMEFISH	NUMBER CAUGHT	TIME CAUGHT	COMMENTS
WAHOO			
DOLPHIN			
BLUEFIN TUNA			
YELLOWFIN TUNA			

REMARKS _____

_____

_____

OCEANOGRAPHIC DATA ACQUISITION FORM

PAGE 1 OF 2 PAGES

FIELD MEASUREMENTS

BOAT NAME

RSS CAL — TIME — DATE

BOAT STATION NO	DATE (DAY, MO)	TIME (LOCAL)	WATER (TEMP)	CHLOROPHYLL SAMPLE SIZE (ML)	SALINITY	AIR (TEMP)	HUMIDITY (DRY, WET)	WIND (DIR, SPEED)	SECCHI (FT)	SEA STATE (FT)	DEPTH (FATHOMS)	SAMPLE (NUMBER)	FU (COLOR)	XBT (Y, N, MODEL NO)	REMARKS
1 2 3	5 6 7 8	10 11 12 13	15 16 17 18	20 21 22 23	25 26 28 29	31 32 34	36 37 39 40	42 43 45 46 47	49 50 51	53 54	56 57 58	60 61 62	64 65	67 68 69 70 71	73 74 75 76 77 78 79 80

OCEANOGRAPHIC DATA ACQUISITION FORM

RELATIVE IRRADIANCE LOG

PAGE 2 OF 2 PAGES

BOAT NAME ____________ INST. NO. ____________

STATION NUMBER	DATE DAY	DATE MO	TIME (LOCAL)	TEST DEPTH (FT)	RELATIVE IRRADIANCE BLUE REL %	RELATIVE IRRADIANCE GREEN REL %	RELATIVE IRRADIANCE RED REL %	RELATIVE IRRADIANCE NEUTRAL REL %	MEASUREMENT POINT	PHOTOMETER ATTN	PHOTOMETER BLUE FT CANDLES	ATTN	GREEN FT CANDLES	ATTN	RED FT CANDLES	ATTN	NEUTRAL FT CANDLES	% CLOUDS OVER BOAT	% CLOUDS OVER AREA	% HAZE	SEA STATE
1 2 3	4 5	6 7	8 9 10 11	12 13	14 15 16 17	18 19 20 21	22 23 24 25	26 27 28 29		30	31 32 33 34	35	36 37 38 39	40	41 42 43 44	45	46 47 48 49	70 71	72 73	74 75	76 77
									DECK READINGS												
									SUBSURFACE READINGS	50	51 52 53 54	55	56 57 58 59	60	61 62 63 64	65	66 67 68 69				
									DECK												
									SUBSURFACE	50	51 52 53 54	55	56 57 58 59	60	61 62 63 64	65	66 67 68 69				
									DECK												
									SUBSURFACE	50	51 52 53 54	55	56 57 58 59	60	61 62 63 64	65	66 67 68 69				
									DECK												
									SUBSURFACE	50	51 52 53 54	55	56 57 58 59	60	61 62 63 64	65	66 67 68 69				
									DECK												
									SUBSURFACE	50	51 52 53 54	55	56 57 58 59	60	61 62 63 64	65	66 67 68 69				
									DECK												
									SUBSURFACE	50	51 52 53 54	55	56 57 58 59	60	61 62 63 64	65	66 67 68 69				
									DECK												
									SUBSURFACE	50	51 52 53 54	55	56 57 58 59	60	61 62 63 64	65	66 67 68 69				
									DECK												
									SUBSURFACE	50	51 52 53 54	55	56 57 58 59	60	61 62 63 64	65	66 67 68 69				

GAMEFISH LOADING FORM

CARD 1

DATE			SQUARE ASSIGNED	NUMBER OF GAMEFISH ENTRIES	BOAT (CODE)	CAPTAIN (CODE)	TIME				NUMBER OF RODS FISHED	ROD HOURS FISHED BAIT					BILLFISH SIGHTED					REMARKS
							LINES IN		LINES OUT								BILLFISH SIGHTED (CD)	TIME 1		TIME 2		
MO	DAY	YR					HR	MIN	HR	MIN		MULLET	BALLYHOO	ARTIFICIAL	STRIP	OTHER		HR	MIN	HR	MIN	
1 2	3 4	5 6	7 8	9 10	11 12 13	14 15 16	17 18	19 20	21 22	23 24	25	26 27 28 29	30 31 32 33	34 35 36 37	38 39 40 41	42 43 44 45	46	47 48	49 50	51 52	53 54	55 56 57 58 59 60 61 62 63 64 65 66 67 68 69 70 71 72 73 74 75 76 77 78 79 80

APPENDIX B

REMOTE SENSING DATA PRODUCTS
SKYLAB
NC130B AIRCRAFT
E-18 AIRCRAFT

SKYLAB DATA PRODUCTS

SENSOR	DATA PRODUCT	DATE RECEIVED	DATA QUALITY	ACTUAL APPLICATION
S190A	70 mm positive and negative transparencies	12-10-73	Good	Attempt to relate film density and gamefish abundance and distribution. Determination of cloud cover.
	9 in. color prints	05-09-74	Good	
	9 in. positive and negative transparencies	05-04-74	Good	
S190B	9 in. color prints	02-12-74	Good	Same as S190A
	5 in. positive transparencies	05-06-74	Good	
S191	Computer compatible tape	06-21-74	Good	Cloud cover too extensive over the .435 Km footprint
	Radiance tabulation	06-11-74	Good	
	Strip charts	02-01-74	—	
S192	Computer compatible tape	01-28-75 and	Problem - High Frequency Filtering	Used in correlation and white marlin distribution modeling.
		06-26-75	Good	
	Color transparencies	12-02-74	Good	
S194	Computer compatible tape	07-02-74	Good	None

NC 130B DATA PRODUCTS

SENSOR	DATA PRODUCT	DATE REC'D	DATA QUALITY	ACTUAL APPLICATION
I^2S	9" positive transparencies	09-10-73	Good	None
AMPS*	9" positive transparencies	09-10-73	Good	Located water rips
RC 8	9" positive transparencies	09-10-73	Roll 11 - poor Roll 20 - good	Located water rips
Recono-fax IV	Film image	09-10-73	Poor. Few water features. Bands across imagery.	None
MSS	Analog Tape	09-10-73	Useless. Syn signals insufficient for decommutation	None
PRT 5	Time/Temperature Listing	10-05-73	Good	Surface Temperature Map

* Imagery received from Houston for only one camera out of the six available.

NASA CONTRACTOR E-18 AIRCRAFT

SENSOR	DATA PRODUCT	DATE AVAILABLE	DATA QUALITY	ACTUAL APPLICATION
Hasselblad 1 and 2	Transparencies	08-27-73	Fair; exposure good for color; poor for IR	Located rips and surface hub vessel
K-17	Transparencies	08-27-73	Good	Located rips and surface hub vessel
E20-D	Computer compatible tape	08-27-73	Good	Chlorophyll and turbidity measurements
	Computer cards			
	Time History			
RS-18	Analog film negative	08-27-73	Good	None
	Radiometer Temperature printout	08-27-73	Good	Surface Temperature Map
PRT 5	Time/Temperature Listing	08-27-73	Good	Surface Temperature Map
	Time History	08-27-73	Poor	


MAR 1976
RECEIVED
NASA STI FACILITY
INPUT BRANCH